Agricultural intensification vs climate change: What drives long-term changes of sediment load?

ShengpingWang[1,2,3*], Peter Strauss[2], Carmen Krammer[2], Elmar Schmaltz[2], Borbala Szeles[3,4], Kepeng Song[1], Yifan Li[1], Günter Blöschl[3,4]

设置格式: 德语(奥地利)
设置格式: 上标, 德语(奥地利)
设置格式: 德语(奥地利)
设置格式: 上标, 德语(奥地利)
设置格式: 德语(奥地利)

1. College of Hydraulic and Hydro-Power Engineering, North China Electric Power University, Beijing, 102206, P.R.China
2. Institute for Land and Water Management Research, Federal Agency for Water Management, A-3252 Petzenkirchen, Austria
3. Institute of Hydraulic Engineering and Water Resources Management, Vienna University of Technology, Vienna, Austria
4. Vienna Doctoral Programme on Water Resource Systems, Vienna University of Technology, Vienna, Austria

***Corresponding author**: Shengping Wang

Email: wangshp418@126.com;Shengping_Wang@ncepu.edu.cn

Abstract: Climate change and agricultural intensification are expected to increase soil erosion and sediment production from arable land in many regions. However, so far, most studies were based on short-term monitoring and/or modeling, making it difficult to assess their reliability in terms of estimating long-term changes. We present the results from a unique data set consisting of measurements of sediment loads from a 60 ha catchment (the Hydrological Open Air Laboratory, HOAL, in Petzenkirchen, Austria) which was observed periodically over a time period spanning 72 years. Specifically, we compare Period I (1946-1954) and Period II (2002-2017) by fitting sediment rating curves for the growth and dormant seasons for each of the periods. The results suggest a significant increase in sediment loads from Period I to

删除: commonly took land use/cover change and landscape structure change as a whole when perofrming such attribution analysis, and most have been
删除: in
删除: has been
删除: window
删除: yield

Period II with an average of 5.8±3.8 t·yr^{-1} to 60.0±140.0 t·yr^{-1}. The sediment flux changed mainly due to a shift of the sediment rating curves (SRC), given that the mean daily discharge significantly decreased from 5.0±14.5 l·s^{-1} for Period I to 3.8±6.6 l·s^{-1} for Period II. The slopes of the SRC's for the growing season and the dormant season of Period I were 0.3 and 0.8, respectively, whilst they were 1.6 and 1.7 for Period II, respectively. Climate change, considered in terms of rainfall erosivity, was not responsible for this shift, because erosivity decreased by 30.4% from the dormant season of Period I to that of Period II, and no significant difference was found between the growing seasons of Periods I and II. However, the change in sediment flux can be explained by the changes in land use and land cover (LUCC) and the change in land structure (i.e. organization of land parcels). At low and median streamflow conditions, land structure in Period II (i.e. the parcel effect) had no apparent influence on sediment yield. With increasing streamflow, it became more important in controlling sediment yield, as a result of an enhanced sediment connectivity in the landscape, leading to a dominant role at high flow conditions. The increase in crops that make the landscape prone to erosion and the change of land uses between Periods I and II led to an increase in sediment flux, although its relevance was surpassed by the effect of parcel structure change at high flow conditions. We conclude that land cover and land use change and land structure change should be accounted for when assessing sediment flux changes. Especially during high flow conditions, land structure change substantially altered sediment fluxes, which is most relevant for long-term sediment loads and land degradation. Increased attention to

删除: 11.6
删除: 10.8
删除: on
删除: 63
删除: 6
删除: 84.0
设置格式: 非突出显示
删除: on
删除: annual
删除: streamflow
删除: varied
设置格式: 字体: 非倾斜
设置格式: 字体: 非倾斜
删除: little between the periods (5.6 *l*·*s*$^{-1}$ and 7.6 *l*·*s*$^{-1}$,
删除: the log regression lines of
删除: 16.72
删除: 4.9
删除: 5.38
删除: 17
删除: given that
删除: changes
删除: crop type
删除: parcel
删除: During
删除: (*i.e.* $Q < Q_{20\%}$)
删除: consolidation
设置格式: 字体: 非倾斜
删除: did not exert
删除: an
删除: production
删除: Whilst
删除: w
删除:
删除: ($Q > Q_{20\%}$)

improving land structure is therefore needed in climate adaptation and agricultural catchment management.

Keywords: **Sediment regime; Land use/cover change; Parcel structure; Climate change; Agricultural catchment**

Introduction

Soil erosion is a phenomenon of worldwide importance because of its environmental and economic consequences (García-Ruiz, 2010; Prosdocimi et al., 2016). Climate change, land use/cover changes (LUCC) and other anthropogenic activities are commonly considered potential agents that drive variation of soil erosion rates (Nearing et al., 2004; Zhang et al., 2021). The impacts of climate change (e.g. Nearing et al., 2004; Zhang and Nearing., 2005; Mullan, 2013; Palazon and Navas, 2016) and of land use and cover change (e.g. Bochet et al., 2006; Korkanç et al., 2018; Nampak et al., 2018; Li et al., 2019; Perović et al., 2018) on erosion have been studied in recent years. As the two agents usually exert their influence on soil erosion simultaneously, their relative contributions have also been increasingly investigated in recent years (e.g. Bellin et al., 2013; Sun et al., 2020; Zhang et al., 2021). Combining field investigations with model simulations, Zhang et al. (2021) quantitatively evaluated the contributions of the decrease in annual rainfall erosivity, the decrease in arable land and bare land, and the construction of silt trap dams to the reduction of sediment load of a typical Loess watershed between 1987-2016, with the contribution

删除: parcel
删除: risk
删除: ing
删除: Jean-Baptiste et al., 2015;
删除: Besides Tt
删除: s
删除: future climate projections or recently observed
删除: on soil erosion have been explored in a number of
删除: Jean-Baptiste et al., 2015;
删除: ; Mullan et al., 2019
删除: . Changes in
删除: the impacts
删除: or
删除: land
删除: (LUCC)
删除: have also been widely investigated, using either
删除: Silva et al., 2017; Bochet et al., 2006; Karvonen et
删除: . Additionally,,,
删除: t
删除: or rolesof climate change and land use/cover
删除: , as both agents usually exert their influence on soil
删除: For example, In a review on anthropogenic and clin
删除: using
删除: combined
删除: ing
删除: climate change
删除: land use
删除: ,
删除: to on
删除: reduction
删除: over

values being +29%, +40%, and +31%, respectively. Scholz et al (2008) modelled how management practices on the local scale would affect soil erosion compared to climate change. They concluded that the conservational management practices would have a greater impact on reducing soil erosion rates than forecasted effects of climate change (i.e. the decrease in rainfall amounts in erosion sensitive months). Also, soil erosion accelerated by livestock grazing was found to be more important than climate change in the Qinghai-Tibet Plateau (Li et al., 2019).

Previous studies provide valuable information on understanding how LUCC and climate change affect soil erosion and sediment load. However, it seems that most of the previous studies considered LUCC (a change in land use and/or types of crops) and landscape structure change (a change in parcel size and structure) together. The relevance of landscape structure changes alone has so far received less attention. However, land use policies, such as land consolidation, have changed agricultural practices to a large extent since 1945, the beginning of agricultural industrialization (e.g. Moravcová et al., 2017; Devaty et al., 2019), and in particular in countries where this process is relatively recent (Bouma et al., 1998; Moravcova et al., 2017; Zhang et al., 2021).

Landscape structures usually influence erosion due to the boundary effects between land uses and land units (parcels) that differ in water and sediment trapping capacity (Baudry and Merriam, 1988; Merriam, 1990; Takken et al., 1999; Phillips et al., 2011). Van Oost et al. (2000) and Devaty et al. (2019) evaluated the role of landscape structure by accounting for its spatial connectivity using modelling approaches and

删除: ,

删除: applied a modeling approach combined with climat

删除: s

删除: ill

删除: with

删除:

删除: the impact of

删除: ,In their work,

删除: found

删除: and

删除: Sun et al. (2020) quantified the contribution of clim

删除: generated a higher impact on soil erosion at the plo

删除: had

删除: ill

删除: controls

删除: the climate changethe decrease in rainfall amounts

删除: effect (Scholz et al., 2008)

删除: livestock grazing accelerated

删除: The p

删除: findings

删除: land use and/or

删除: or

删除: /or

删除: for implementing water and soil conservation meas

删除: ly

删除: commonly took

删除: as a whole to understandit'stheir role oin affecting

删除: ,in either attribution analysis or studies with

删除: not

删除: much

删除: ,

删除: even

删除: though

删除: -

found that landscape structure is an essential factor when assessing the risk of soil erosion affected by land use changes. Both studies emphasized the potential impacts of land parcel structure changes on sediment production through altering hydrological and sediment connectivity. However, both studies relied on models, making connectivity assumptions in their studies. Instead of focusing on the spatial connectivity, others (e.g. Bakker et al., 2008; Sharma et al., 2011; Chevigny et al., 2014; Wang et al., 2021; Tang et al., 2021; Madarász et al., 2021) evaluated the effect of terrain, soil properties, lithology, management practices and other processes associated with landscape and/or land structure changes and highlighted their impact on sediment production. It has also been shown that the impact of landscape structure on erosion is more heterogeneous when different crops are grown, and the underlying lithology, soil properties and topography show substantial spatial variability across the catchment (David et al.,2014; Cantreul et al., 2020).

In our analysis, we evaluate the relative roles of climate change, LUCC and the change of land structure on sediment production. We define LUCC as a change in either type of land use (i.e. arable land, grassland, forest) or type of land cover (agricultural management, mainly by crops with different risk of soil erosion). We focus on understanding the respective role of LUCC and landscape structure change, based on long term observations that were usually not available in previous studies. We present the results from a unique data set consisting of measurements of sediment loads from a small agricultural catchment over a time window of 72 years. The study catchment is the 66 ha Hydrological Open Air Laboratory (HOAL) located in

删除: -

删除: Even though numerous studies have addressed the effect of climate change and land management on soil erosion and sediment production, most studies have been based on short-term monitoring and/or modeling, which makes it difficult to assess their reliability in terms of long-term changes that are the most relevant from a practical perspective.

删除: This paper

删除: aims at evaluating

删除: land use and land cover changes

删除: (LUCC)

删除: ,

删除: especially with the

删除: f

删除: the basis of a

删除: n

删除: time frame

删除: of

删除: are

删除: usually

删除: commonly

删除: absent

删除: most of the

删除: analysis

删除: p

删除: potentially spanning

Petzenkirchen (Blöschl et al., 2016), which, in addition to being exposed to climate change, has experienced a significant change in land use and land cover as well as parcel structure due to changes in land management policies during the past decades. Both discharge and suspended sediment concentration have been monitored periodically in the HOAL catchment from 1945 to 1954 and from 2000 to now. This provides an opportunity to disentangle the impacts of land structure change, land use/land cover change, and climate change based on long-term measurements. Specifically, we aim at i) exploring how the sediment regime shifted between the periods of 1945-1954 and 2002-2017; ii) analyzing whether climate change or LUCC (or both) were responsible for any change in the sediment regime; and iii) identifying the relevance of land structure change (i.e. land consolidation) on erosion control compared to LUCC.

2. Methods

2.1 Catchment characteristics

The HOAL catchment is situated in Lower Austria's alpine forelands (48°9' N, 15°9' E) with elevations ranging from 268 m to 323 m a.s.l. and a size of 66 ha (Figure 1). The climate of the catchment belongs to the temperate, continental climate zone (Dfb) according to Köppen-Geiger (Kottek et al., 2006). The mean annual precipitation is 746 mm (1946 - 2006), 62% of the rain falling between May and October. The mean daily air temperature is 8.8°C (1946-2006). The dominant land use is arable land, accounting for on average 82% of the catchment land use over the past few years. Typical crops include winter wheat, corn and barley. Deciduous trees grow along the

删除: for erosion control
删除: an
删除: altered
删除: y
删除: yield
删除: since the 1940s
删除: for
删除: ing
删除: parcel
删除: and
删除: the
删除: the impact of
删除: has change
删除: d
删除: 1946
删除: land-use changes
删除: any
删除: that of a change in land use or cover
删除: ,
删除: with a
删除: of
删除: ,
删除: and t
删除: ,
删除: ,

stream (6%), 10% of the area is grassland, and 2% is paved. The subsurface of the catchment consists of tertiary marine sediments. Soils are classified into five types: calcic cambisols, vertic cambisols, gleyic cambisols, planosols and gleysols (IUSS Working Group WRB, 2015).

2.2 Data availability

Both discharge (Q, l/s) and suspended sediment concentration (C, mg/l) have been measured at the catchment outlet periodically since the 1940s. A data set of discharge and sediment concentration was available for the period 1945-1954. After that, measurements were stopped and started again in 1990. Therefore, data records for the period 1946-1954 (Period I) and 2002-2017 (Period II) were used for this analysis. In Period II, the stream gauge was relocated. However, the difference in catchment size is very small (around 200 m^2). This is indicated by the different locations of the discharge gauge in Figure 1. Due to technological advances, the measurement method of both Q and C changed between the two periods. In Period I, discharge was registered by a Thompson weir and a paper chart recorder, while in Period II, it was registered by an H-Flume and a pressure transducer. Thus, high temporal resolution, one-minute data for discharge were available for both periods. Sediment concentrations were measured manually every 3-4 days in Period I, whilst an automatic method (i.e. equal-discharge-increment sampling) and additional manual sampling were applied in Period II. Daily precipitation and 5-min rainfall intensities were available for both periods, but for Period I, 5-min rainfall intensities were only available during the growing season.

删除: creek
删除: streamflow
删除: D
删除: time between
删除: only
删除: ,
删除: Sso
删除: D
删除: from
删除: to
删除:
删除: available
删除: Because, to our knowledge, for theperiod of time
删除: S
删除: were
删除: in Period II
删除: size of
删除: between the two periods
删除: .
删除: ,
删除: , which is barely visible on the map
删除: and
删除: measuring
删除: .
删除: D
删除: the data was
删除: were measured with
删除: different
删除: methods
删除: at 10 min resolution
删除: at 5 min resolution
设置格式: 字体: 非倾斜
删除: (EWDI)
删除: plus

We used parcel-based land use data from 1946 to 1949 and 2007 to 2012, representing Period I and Period II land use, respectively. Land use categories were agricultural land, including crop type, grassland, forest, roads and settlements (i.e. paved area). We defined a parcel as a continuous area of land with a single crop type. Parcel boundaries were specified according to the cadastral map and aerial photographs. In Period II, these boundaries were also visually inspected. Figure 1 depicts the geographic catchment location, and parcel structure and land use for a specific year in each period.

设置格式: 字体: 非倾斜

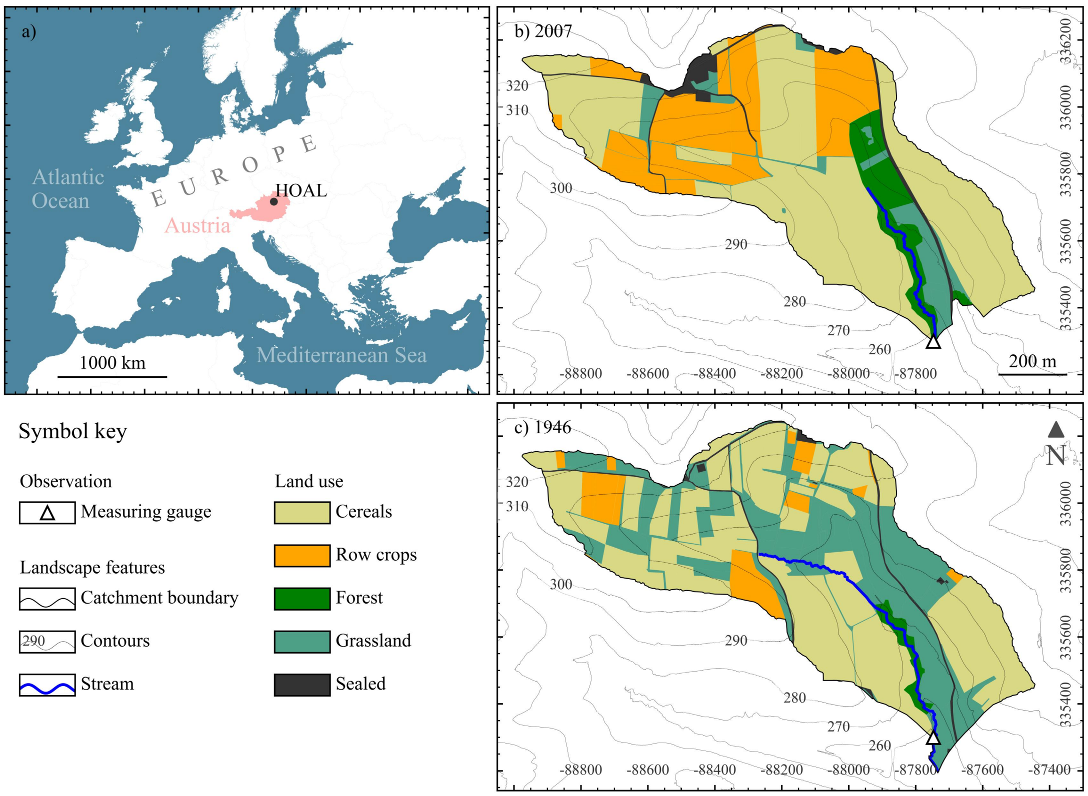

Figure 1 Geographical location of the HOAL catchment in Petzenkirchen in Austria and Europe (a) and Parcel structure and land use in the HOAL catchment for 2007 (b) and 1946 (c). Coordinates as EPSG: 31256 – MGI / Austria GK East (meters).

删除: **1947**

删除: **a**

删除: **2007**

删除: **b**

删除: **The black hatched area in b) represents a difference in catchment size due to the relocation of the stream gauge in Period II**.

2.3 Data analysis

2.3.1 Changes in rainfall erosivity and flow regime

The erosive potential of rainfall events was quantified by the R-factor of the Revised Universal Soil Loss Equation (RUSLE), which is defined as the product of kinetic energy of a rainfall event and its maximum 30-min intensity, using the rainfall erosivity tool RIST (USDA-Staff, 2019) according to

$$EI_{30} = \sum_{i=1}^{m} E_i \cdot I_{30,i} \qquad (1)$$

where EI_{30} is the Annual R-factor (MJ·mm ha^{-1}·hr) calculated as the sum of single event R-factors, E_i is the total kinetic energy for a single event (MJ·m^{-2}), I_{30} is the maximum rainfall intensity in 30 minutes within a single event *i* (mm·h^{-1}), and *m* is the number of events per year.

We assumed erosivity density *ED* (i.e. EI_{30} divided by event precipitation) to be a particularly relevant climatic indicator of soil erosion process and catchment sediment yield, because it is calculated as a combination of rainfall kinetic energy and maximum rainfall intensity of rain events. These are commonly considered as the relevant parameters of rain to trigger soil erosion. We thus tested whether the means of the monthly erosivity density (*ED*) are significantly different between Period I and Period II by using a t-test. Due to the absence of rainfall intensity measurements, we could not directly calculate *ED* for the months of the dormant season (November to March) of Period I. Instead, we calculated *ED* from a relationship between EI_{30} and monthly rainfall of Period II, assuming that the relationship was sufficiently temporally invariant over the investigated periods. Erosivity density is very low

删除: effect
删除: on erosion
删除: N.h-1.yr-1
设置格式: 非上标/ 下标
设置格式: 非上标/ 下标
设置格式: 非上标/ 下标
设置格式: 字体: （默认）Times New Roman, 小四
删除: *
设置格式: 字体: （默认）Times New Roman, 小四
设置格式: 字体: （默认）Times New Roman, 小四
删除: /
设置格式: 字体: （默认）Times New Roman, 小四
设置格式: 上标
删除: *
设置格式: 字体: （默认）Times New Roman, 小四
删除: kJ
设置格式: 字体: 非倾斜
删除: the
删除: the
删除: process
删除: ,
删除: ,
删除: according tousing the high rainfall intensity dataset
删除: For this caseRather

during the dormant season. The mean *ED* was 0.66±0.21 and 2.54±2.43 MJ· ha^{-1}· hr^{-1} respectively for the dormant season and the growing season of Period I, whilst it was 0.42±0.11 and 1.87±1.35 MJ ·ha^{-1} ·hr^{-1} respectively in Period II (Figure 3a). Thus, the error arising from the use of this relationship is expected to be small.

We also compared daily flow duration curves to understand whether hydrological regime change has influenced flow transporting capacity and sediment regime change. Following the definitions of Smakhtin (2001), we compared low flow ($Q_{70\%}$), high flow ($Q_{10\%}$) and median flow rate ($Q_{50\%}$) quantiles for the two periods.

2.3.2 Sediment regime analysis

To analyze sediment regime, we first estimated sediment loads for the different periods. After calculating SRCs for Period I and Period II, using the data pairs of *Q* and *C* measurements, daily sediment load was estimated (see equation 2) by combining the measured high resolution data (1 min) for *Q* with the derived SRC for each period. For further analysis, the daily sediment load was aggregated either by month or year.

$$Y = \sum Q_i \cdot \hat{C}_{i\_s} \cdot T_i / 1000000 \qquad (2)$$

where *Y* is the sediment load within a day (kg·day^{-1}), Q_i is the observed discharge at time step *i* (l·s^{-1}); $\hat{C}_i$ is the estimated sediment concentration at time step *i* (mg·l^{-1}). T_i (s) is the elapsed time between time step *i* and the next time step *i*+1. The statistical differences of sediment loads either between seasons or between periods were examined by a t-test.

- 删除: (
- 删除: t
- 删除: l
- 删除: r
- 删除: l
- 删除:)
- 删除: ;
- 删除: t
- 删除: variation
- 删除: In order
- 设置格式: 非突出显示
- 删除: t
- 删除: z
- 设置格式: 非突出显示
- 删除: W
- 删除: ly
- 删除: firstly
- 设置格式: 非突出显示
- 删除: winthin
- 删除: time
- 删除: estimating
- 设置格式: 非突出显示
- 删除: on of
- 删除: sediment rating curves (
- 删除:
- 设置格式: 非突出显示
- 删除:)
- 设置格式: 非突出显示
- 删除: respectivelly, according to the original
- 设置格式: 非突出显示
- 设置格式: 非突出显示
- 设置格式: 字体: 倾斜
- 设置格式: 字体: 倾斜
- 设置格式: 非突出显示

Following a commonly used approach (Asselman, 2000; Warrick and Rubin, 2007; Sheridan et al., 2011; Vaughan et al., 2017; Khaledian et al., 2017), the SRCs were here assumed to follow a power-law function, which was fitted by least squares regression:

$$C = a \cdot Q^{b} \qquad (3)$$

where C is sediment concentration ($mg \cdot l^{-1}$), Q is discharge ($l \cdot s^{-1}$), and a and b are regression coefficients. The coefficient a is usually associated with easily transported intensively weathered materials and may vary over seven orders of magnitude (Syvitski et al., 2000). The parameter b represents the capacity of the stream to erode and transport sediment, reflecting how sediment concentration is non-linearly related to streamflow (Sheridan et al., 2011; Fan et al., 2012). It typically varies from 0.5 to 1.5 and rarely exceeds 2. Sometimes b is also regarded as a measure of the quantity of newly available sediment sources (Vanmaercke et al., 2010; Guzman et al., 2013). Considering that data records were registered with different intensity for Periods I and II (see section 2.2), for the sake of consistency, we used monthly averages, as in other studies (Syvitski and Alcott,1995; Sheridan et al., 2011; Hu et al., 2011), to construct SRCs. We assumed that monthly averages could reflect a varied hydrological and/or sediment response to seasonally prevailing weather characteristics such as dry periods or convective storms (Sheridan et al., 2011).

We chose arithmetic means of the observations to represent the monthly Q and C values. These monthly averages were pooled together and then grouped into growing season of Period I (Period I_G), dormant season of Period I (Period I_D), growing

删除: Sediment regimes were mainlyare also usually analyzed using sediment rating curves (SRC).

删除: 2

设置格式: 字体: 非倾斜

设置格式: 字体: 非倾斜

删除: dimensionless

删除: available

删除: temporal resolutions

删除: See

删除: conducted

删除: the

删除: ’

season of Period II (Period II_G), and dormant season of Period II (Period II_D), respectively. For each of these four periods, we fitted SRC.

We analyzed the fitted SRC by two strategies to evaluate whether and how the sediment regime changed between these periods. Besides directly comparing the slopes of the four seasonal SRCs by ANCOVA analysis with the log-transformed discharge as indipendent variable, we also fitted the SRC for each specific year's season and plotted the regression coefficients *a* against their corresponding *b* to evaluate a possible sediment regime shift during Periods I and II.

The latter framework was adapted from Thomas (1988), and also employed by Asselman et al. (2000) and Fan et al. (2012) to examine differences in sediment regimes between spatially different sites. Also, Sheridan et al. (2011) used the framework to reveal post-fire temporal shifts of a sediment regime. Thomas (1988) suggested that time-based sampling methods (either random sampling or systematic sampling) preferentially use observations of relatively small discharges to fit a SRC. This tendes to reduce the slope and increase the intercept of a SRC (see point C in Figure 2b). In contrast, flow-based automatic sampling methods such as equal-discharge-increment sampling preferentially use observations of relatively large discharges. Thus, they tend to cause a reversed pattern of *a* and *b* (i.e. increase the slope and decrease the intercept of SRC, see the point A in Figure 2b). However, irrespective of sampling practices, the pairs of data points *a* against *b* will likely be allocated along a straight line, if sediment transport regimes are similar. The reason for the *a*-*b* pairs lying nearly on a straight line is mainly due to a mathematical

删除: covariate
删除: and year
删除: Thomas (1988) suggested that this technique could
删除: was originally mentioned in the research ofi
设置格式: 非突出显示
设置格式: 非突出显示
删除: in which the authorssuggested that
设置格式: 非突出显示
删除: commonly
删除: makes
删除: of
删除: magnitude of
删除: for
删除: ting
删除: ,
删除: ing
删除: S
删除: the
删除: (
删除:)
删除: ;
删除: whilst
设置格式: 非突出显示
删除: (For example,
删除: EWDI
删除:)
删除: select
删除: magnitude of
删除: ,
设置格式: 非突出显示
设置格式: 非突出显示
删除: ing
设置格式: 字体: 非倾斜
删除: (

property. That is, the slopes could be expressed by a linear function of the intercepts with the coordinates of the common point (Thomas, 1988). Therefore, for years with similar means of log-*Q* and log-*C*, the SRCs will pass through one common point O (Thomas, 1988; Syvitski et al.,2000; Desilets et al., 2007; Sheridan et al., 2011). This common point O (Figure 2a) is usually interpreted to reflect time invariant catchment characteristics, such as relief, drainage area, and drainage density, while the variation of the slope of SRCs (Figure 2a) is interpreted to reflect temporally dynamic characteristics, such as average or maximum discharge and sediment availability (Asselman, 2000). The coefficients *a* are usually inversely linearly related to *b* (Thomas, 1988, Syvitski et al., 2000 and Desilets et al., 2007), and each point is representative of a period (or a catchment). If sediment transport regimes are similar between periods (catchments), the points will be plotted on the same line (such as A, B, C in Figure 2b), with points A of Figure 2b (upper-left-side) often exhibiting steeper sediment rating curves than points C (lower-right side). As for different lines in Figure 2b, the lower ones characterized by points A', B', and C' represent situations with most of the annual sediment load being transported at relatively low flow discharges. Whilst the higher ones characterized by A, B, and C represent situations with suspended sediment being mainly transported at high streamflow. Compared to a direct evaluation of rating curves, relating coefficient *a* to exponent *b* is more conductive to revealing temporal evolution of sediment regime (Syvitski et al., 2000; Desilets et al., 2007). The change in the relationship of coefficients *a* against *b* between the periods was also examined by ANCOVA.

删除: ,
删除: t
删除: The reason behind this could be partly explained by
删除: n
删除: ir
删除: parameters of
删除: t
设置格式: 非突出显示
删除: .
删除: , which causes that the pairs of point of ***a*** and
设置格式: 字体: 加粗
设置格式: 字体: 加粗
删除: Detailed understandingon the framework could be
删除:
删除: f
删除: the
删除: (or catchments)
设置格式: 字体: 倾斜
设置格式: 字体: 倾斜
删除: would usually
删除: of the SRCs having a common point
删除: with
删除: as well
删除: This provides a means for testing whether periods (
删除: (
删除:)
删除: are representative of periods (or catchments) havi
删除: . P
删除: usually
删除: F
删除: position of the
删除: the
删除: ,
删除: and

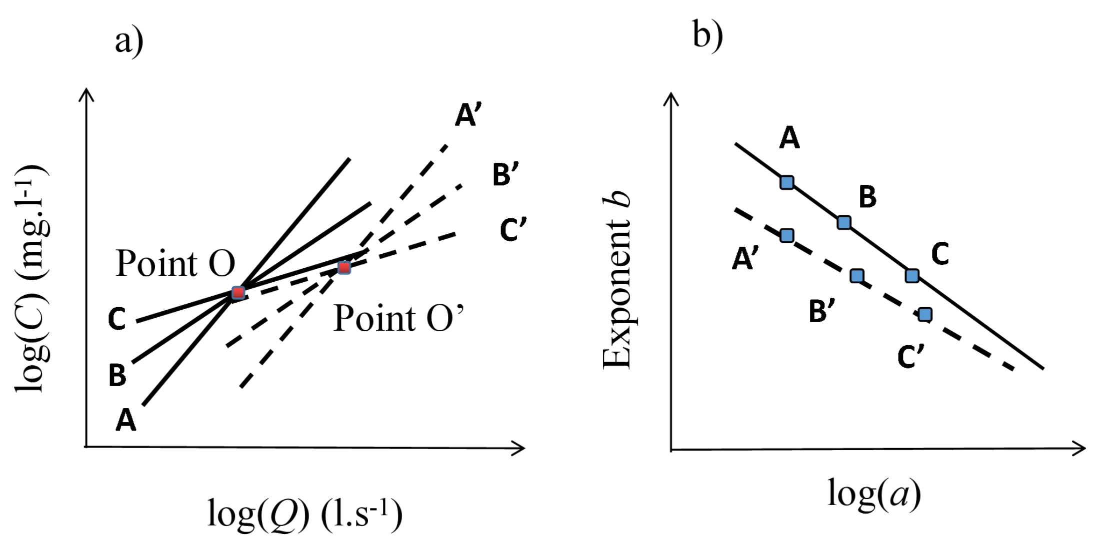

Figure 2 Schematic showing a) how sediment rating curves (SRC) may rotate around a common point and b) how exponents *b* of the SRC relate to coefficients *a*. Lines A, B and C on the left are SRC of different periods (e.g. years) sharing a similar common point O. Once sediment regimes shift due to the changes in catchment characteristics (change in drainage density, drainage area, and topography) the common point O would change to point O', and the linear relationship between *a* and *b* of the SRC would exhibit a shift as well. The schematic is based on log *C* =log *a* + *b*·log *Q* (Equation 3).

To account for uncertainties of the fitted SRC during each period, we additionally established theoretical sediment rating curves (tSRC)

i) For each period (i.e. Period I_G, Period I_D, Period II_G, and Period II_D), we carried out random sampling of *log a* (n=500, package "sample" in R), assuming that the samples of the coefficient of log *a* follow normal distributions, which was examined with a Kolmogorov-Smirnov test of normality (mean = 1.02, SD = 2.01, n=44, p<0.05);

删除: .....

删除: 2

删除: ;

删除: i) f

设置格式: 编号 + 级别: 1 + 编号样式: i, ii, iii, ... + 起始编号: 1 + 对齐方式: 左侧 + 对齐位置: 1.1 毫米 + 缩进位置: 1.1 毫米

设置格式: 项目符号和编号

设置格式: 字体: 非倾斜

删除: Studio

删除: (Figure 4)

删除: proved

设置格式: 字体: 倾斜

删除: =??????

ii) Given the set of the sampled 500 values of log *a*, we generated a set of values *b* according to the previously established linear relationship between log *a* and *b*;

iii) Given a set of specified *Q* values, we derived 500 tSRC for each period, corresponding to the paired log *a* and *b* samples;

iv) Using these tSRC we calculated the 50 percentile, the 5 percentile, and the 95 percentile for each period to estimate the uncertainties of the sediment rating curves.

The tSRC of the periods were also used to quantify the effect of land consolidation, i.e. the change of parcels structure and sizes (Parcel_effect) and the effect of land use and land cover changes (LUCC_effect). Vegetation usually plays a minor role in the dormant season due to the absence of a dense vegetation cover on arable land and little erosive rainfall (Madsen et al., 2014; Kundzewicz, 2012; Salesa and Cerda, 2020; Hou et al., 2020). Therefore, landscape structure in the dormant season was considered a dominant factor for water and sediment transfer across the land surface, and thus runoff production and sediment production (Sharma et al., 2011; Devátý et al., 2019). Therefore, we hypothesized that the total change in sediment yield (Total_effect) resulted from land cover change (LUCC_effect), land structure change (Parcel_effect) and climate change (Climate_effect). Since the area of our catchment is only 0.66 km^2, no obvious change was found in the shape of the small stream for the two periods. Stream sediment resuspension is rather small (Eder et al., 2014), therefore, the contribution of bank erosion was not taken into account. The effects of land cover and land structure change was quantitatively separated according to the seasonal differences in tSRC after determining the climate change effect. Specifically,

删除:

删除:

设置格式: 缩进: 左侧: 1.1 毫米

删除: g

设置格式: 缩进: 左侧: 1.1 毫米

删除: iii) g

设置格式: 字体: 倾斜

删除:

删除: u

删除: to

删除: reveal

设置格式: 字体: 非倾斜

删除: versus

删除: SinceSince v

删除: ,

删除: considered

删除:

删除: critically importantdeterminant

删除: affecting

删除: thus

删除: Since

删除: 7

删除: , no

删除: was

删除: .

删除: , andS

删除: was rarely observed

删除: considered to be

删除: winthin the stream

删除: herein

删除: could be

we assumed that the shift of sediment regime from Period I_D to Period II_G was representative of the Total_effect (Equation 4), and the shift in sediment regime between Period I_D and Period II_D was mainly due to land consolidation (Parcel_effect) (Equation 5). The LUCC effect, thus, could be estimated according to Equation (6) if the Climate_effect was insignificant (section 3.1). The contributions of Parcel_effect and LUCC_effect to the Total_effect were estimated according to Equations (7) and (8), respectively.

删除: is
删除: 3
删除: i
删除: 4
删除: Thus, t
删除: 5
删除: 6
删除: 7

$$\text{Total\_effect} = tSRC_{50\%}(\text{Period II\_G}) - tSRC_{50\%}(\text{Period I\_D}) \quad (4)$$

$$\text{Parcel\_effect} = tSRC_{50\%}(\text{Period II\_D}) - tSRC_{50\%}(\text{Period I\_D}) \quad (5)$$

$$\text{LUCC\_effect} = \text{Total\_effect} - \text{Parcel\_effect} - \text{Climate\_effect} \quad (6)$$

$$\text{Parcel\_effect}(\%) = \frac{\text{Parcel\_effect}}{\text{Total\_effect}} \times 100 \quad (7)$$

$$\text{LUCC\_effect}(\%) = \frac{\text{LUCC\_effect}}{\text{Total\_effect}} \times 100 \quad (8)$$

删除: 3
删除: 4
删除: 5
删除: 6
删除: 7

3. Results

3.1 Changes in climate and flow regime

Because climate change is often found responsible for hydrological change (e.g., Kelly et al., 2016; Wang et al., 2020), we compared erosivity density (*ED*) and monthly precipitation (*P*) of the two periods to examine whether climate affected the variation of the sediment regime in the catchment (Figure 3). The mean monthly *ED* in the growing season were 2.37±1.38 and 1.84±0.86 MJ·ha^{-1}·hr^{-1} for Periods I and

删除: commonly
设置格式: 字体: 倾斜
删除: *s*
删除: .
删除: .

II, respectively (Figure 3a). No significant difference (p>0.05) was found between the two growing seasons. Mean monthly *ED* in the dormant seasons showed a significant (p<0.05)

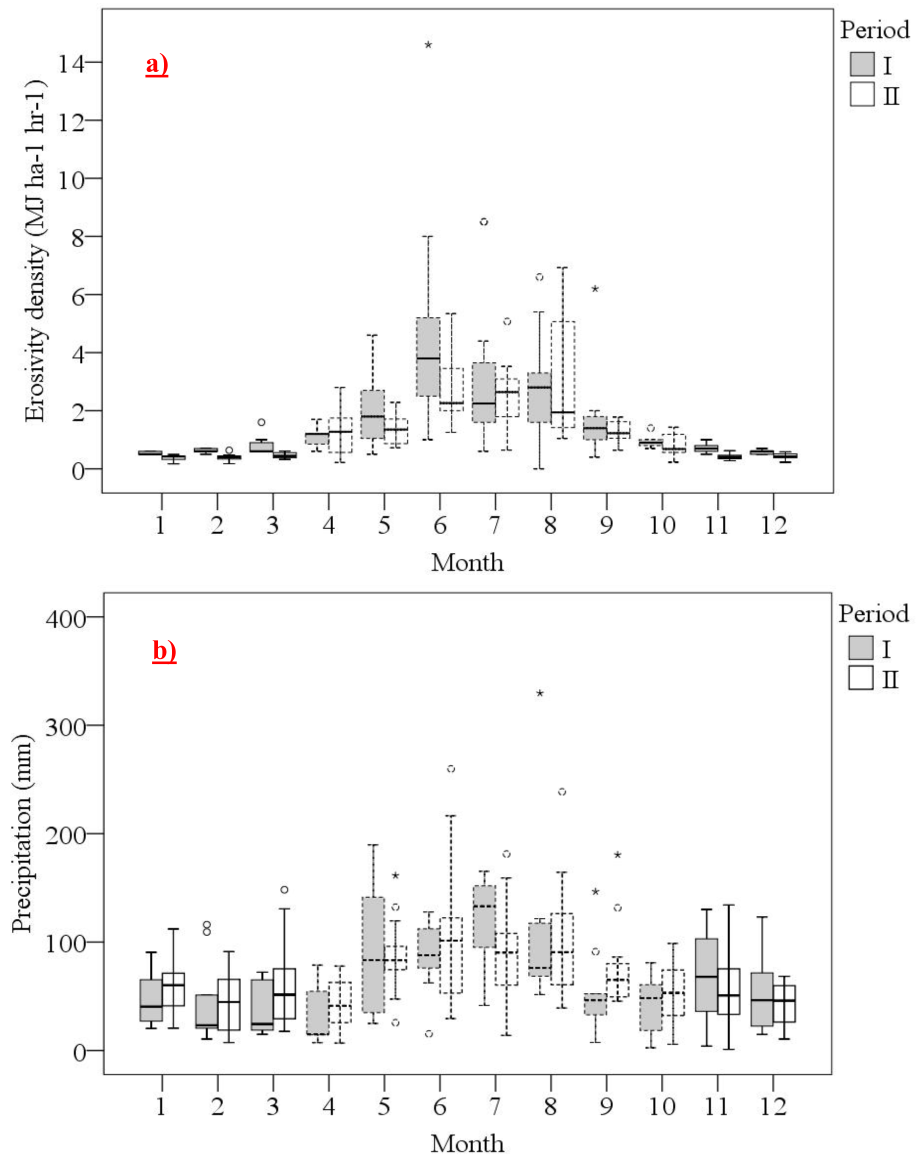

Figure 3 Monthly erosivity density a) and monthly precipitation b) for Periods I and II. The bars with a dashed outline represent the growing seasons (April to October), the bars with a solid outline the dormant seasons (November to March). The whiskers indicate the range between the minium and the maximum, the asterisks indicate the outliers.

删除: $(N{\cdot}h^{-1}{\cdot}yr^{-1}{\cdot}mm^{-1}$

删除:) (standard deviation between years),

删除: ,

删除: which was n

删除: t

删除: ly

删除: t

删除: first and two periods

删除: .

删除: **Distribution of a) m**

删除: **b)**

删除: **whilst**

删除: **meanrepresent**

设置格式: 非突出显示

设置格式: 非突出显示

设置格式: 非突出显示

设置格式: 非突出显示

设置格式: 非突出显示

decrease from the first to the second period (0.66±0.21 and 0.42±0.11 (MJ·ha^{-1}·hr^{-1}), respectively). A *t*-test suggests that there was no significant (p>0.05) difference in mean monthly *P* between the first and second periods in both the dormant and the growing seasons (Figure 3b). The mean monthly *P* was 50±33 and 76±54 mm for the dormant and growing season of Period I, and it was 53±29 mm and 79±47 mm for the two seasons of Period II. The decrease in *ED* during the dormant season of Period II and the insignificant change in monthly *P* suggest that climate change between Period I and II was not responsible for an increased sediment load (see section 3.3). It should be noted, that processes related to snow play a minor role in the catchment because it is considered a lowland catchment, located in a region with very small amounts of snowfall (about 10% of annual rainfall). Thus, a possible change in the proportion of snowfall in precipitation during the winter season of Periods I and II was not accounted for when addressing the impact of climate change on sediment load.

Streamflow in Period I was higher than that of Period II, and the mean annual streamflow was 188 and 146 mm yr^{-1} for Periods I and II, respectively. Daily flow duration curves for both periods are displayed in Figure 4. A t-test suggests that they are significantly different (p<0.05). The $Q_{70\%}$ low flow of the two periods was 2.7 and 2.4 l·s^{-1}, the $Q_{50\%}$ median flow was 4.0 and 3.1 l·s^{-1}, and the $Q_{10\%}$ high flow was 10.7 and 7.5 l.s^{-1}, for the two periods, respectively. The decreased flow regime of Period II, which is probably in part due to an increased evapotranspiration over the past decades (Duethmann and Blöschl, 2018), indicates that streamflow cannot account for the

设置格式: 左, 孤行控制, 定义网格后自动调整右缩进
删除: .
删除: .
删除: second period (Figure 3a). In contrast, mean month
删除: N
设置格式: 字体: 倾斜
删除: was found
删除: for the mean monthly P
删除: either
删除: or
删除: in Period I
删除: in
删除: , respectively
设置格式: 字体: 倾斜
删除: availability
删除: ,
删除: because our investigated
删除: is a
删除: quite
删除: driving sediment transport for only avery few events.
删除: , we think that snowfall in the catchment plays a mi
删除: precipitation
删除: to
删除: snowfall
删除: in
删除: <sp>

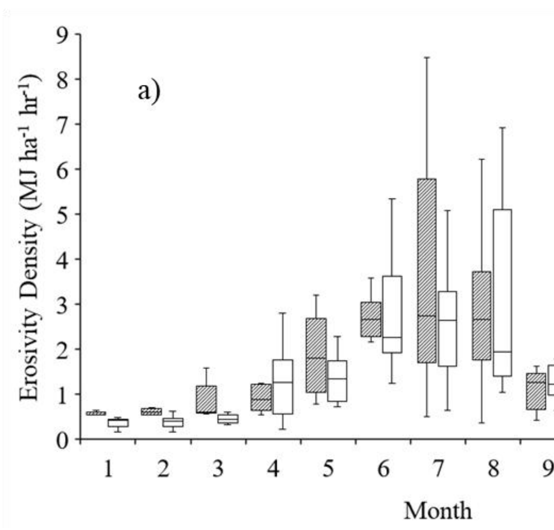

observed increased sediment load of Period II. Otherwise an increased streamflow would be expected in Period II.

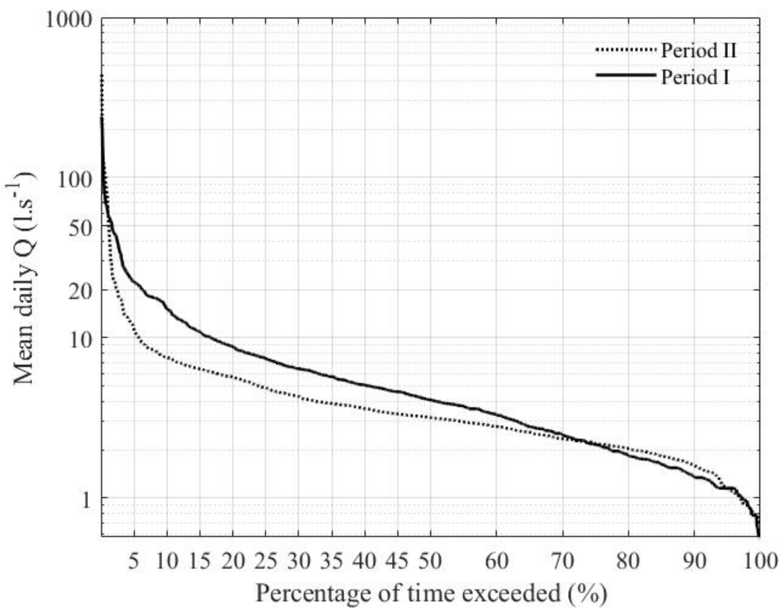

Figure 4 Mean daily flow duration curve for Periods I (solid line) and II (dashed line).

3.2 Change in land use and land organization

Table 1 shows how land use changed between the two periods. During Period I, cropland and grassland accounted for 73% to 82% (varying between years) and 14% to 22%, respectively. However, due to agricultural intensification, cropland increased to around 82% in Period II, at the expense of a decreasing share of grassland. Forest, including sparse forest, accounted for 1.8% area during Period I but increased considerably until Period II to around 11%. The increase in cropland and forest suggests higher rates of evaporation and transpiration, and consequently less streamflow, which is in line with the previously examined trends of of streamflow

删除: transport

删除: in

删除: (see section 3.3)

删除: ,

删除: o

设置格式: 字体颜色: 自动设置

删除: 45

删除: iedinacross the specificdifferent

删除: of the area

删除: Both

删除: ,an

删除: means

删除: an increase in

删除: a

删除: end

删除: accordingly

删除: was

删除: actually

删除: dynamics

dynamics. When further analyzing the land use classes of arable land, a substantial change was found for the crop types too, with the crops of low risk for soil erosion being replaced with crops that exhibit a high soil loss potential. This was particularly true for maize. In addition, the diversity of crops decreased considerably (Table 2). This shift towards agricultural uniformity likely acts as a land structure effect. A loss of heterogeneity of crop types increases the probability that different fields are managed with the same crop. Then even smaller fields may behave similarly to larger fields in terms of sediment production.

Besides the change in land use, the parcel structure of the catchment has also changed (Table 1). This change was related to a land consolidation plan issued in 1955 in Austria (Devátý et al., 2019) and a massive trend to agricultural industrialization that evolved after 1945 (mainly referring to the massive application of advanced machinery and fertilization technologies that started in the 1950s). During Period I, arable land was fragmented across many small parcels, with a mean parcel size between 0.5 - 0.6 ha and a resulting parcel density (number of parcels per ha area) between 1.7 - 2.0 ha^{-1} in different years. In Period II, these values increased considerably to mean parcel sizes between 1.7 - 2.7 ha and parcel densities between 0.3 - 0.6 ha^{-1}. Similarly, the mean parcel size and parcel density of grassland during Period I were 0.13 - 0.17 ha and 5.2 - 7.2 ha^{-1}. It changed to 1.06 ha and 0.9 ha^{-1} in Period II. As parcel structures are identified to influence sediment loads mainly due to the boundary effects (e.g. Baudry and Merriam, 1988;Takken et al., 1999; Phillips et

删除: looking
删除: at
删除: with
删除: s
删除: ,
删除: from
删除: with
删除: to cause
删除: of
删除: changed
删除: to
删除: the
删除: with
删除: of
删除: appeared
删除: This shift to agricultural uniformity is likely to affect also land structure effects
删除: is
删除: to
设置格式: 非突出显示
删除:
删除: right
删除: had
删除: increasingly found
删除: having a role on
删除: ing

al., 2011), the substantial decrease in parcel density of the catchment in Period II, was expected to affect sediment load as well.

删除: i

删除: and the increase in parcel size

删除: ,

删除: also assumed to greatly

Table 1 Parcel and land use statistics for Periods I and II. Land use for the years 1946 to 1949 represents Period I, land use for the years 2007 to 2012 represents Period II; *N* is the number of parcels for a given land use, density is the number of parcels per ha, mean size represents the mean area of parcels with a particular land use.

设置格式: 字体: 倾斜

Parcel Structure								
	Period Ⅰ				Period Ⅱ			
Land use	Parcel number (*N*)	Density ($1 \cdot ha^{-1}$)	Mean size (ha)	Area (%)	Parcel number (*N*)	Density ($1 \cdot ha^{-1}$)	Mean size (ha)	Area (%)
Arable land	70-111*	1.7-2.0	0.5-0.6	73-82	21-33	0.3-0.6	1.7-2.7	81-82
Grassland	70-81	5.2-7.2	0.1-0.2	14-22	6	0.9	1.1	3-4
Forest	1	-	1.2	1.8	7	1	1.0	10.5-11
Paved area	17	12.9	0.1	2	17	7.3	0.1	2.4

* The number of parcels varied with the specific year of a period

带格式表格

设置格式: 字体: 倾斜

设置格式: 字体: 倾斜

Table 2 Crop statistics of arable land for Periods I and II; Crop statistics for the years 1946 to 1949 represent Period I, crop statistics for the years 2007 to 2012 represent Period II; Erosion risk for a particular crop is classified as high or low according to the classification of management in the RUSLE. The statistical values represent the ranges of the area for each crop during Periods I or II.

设置格式: 非突出显示

Crop	Period Ⅰ		Period Ⅱ		Erosion risk
	Area (ha)	Area (%)	Area (ha)	Area (%)	
Meadow	9-15	18-30	0.8	2	low
Alfalfa	11-18	22-33	-	-	low
Wheat	5-14	9-26	3-35	5-66	low
Rye	3-13	5-24			low
Beets	2-12	3-22	-	-	high
Oats	2-10	4-18	2	4	low
Barley	0.3-8	5-15	2-29	5-55	low
Potatoes	3-7	6-14	-	-	high
Maize	0.3-0.8	0.6-1.1	6.3-34	12-63	high
Rape	-	-	0.7-23	1-43	low
Sunflower	-	-	0.2-2	0.3-4	high

设置格式: 居中

带格式表格

设置格式: 居中

3.3 Change in sediment transport regime

3.3.1 Direct comparison of the fitted SRCs

Figure 5 shows the fitted sediment rating curves (p<0.05) for both periods. A t-test suggests that the slopes of the regression lines are significantly (p<0.05) different between the dormant seasons or growing seasons. Although rainfall erosivity of Period II_G was similar to that of Period I_G (Figure 3a) and streamflow of Period II was generally lower than that of Period I (Figure 4), the fitted SRC of Period II_G was steeper than that of Period I_G (Figure 5a), with the coefficients b being 0.3 and 1.6 for Period I_G and Period II_G, respectively (Table 3). The fitted SRC of Period II_D demonstrated a faster response of sediment concentration to increasing flow compared to that of Period I_D (Figure 5b), the coefficients b being 0.8 and 1.7 for Period I_D and Period II_D, respectively. However, the rainfall *ED* in Period II_D was generally lower than that of Period I_D (Figure 3a). This suggests a lower probability of a substantial increase in sediment availability. These results indicate that neither changes in rainfall erosivity nor the hydrological regime could explain the increase in sediment dynamics.

删除: 56
删除: .
删除: T
删除: ANCOVA
删除: were
删除: A
删除: 45
删除: 56
设置格式: 字体: 非加粗
删除: 2
删除: 65
删除: rating curves of the dormant season
删除: s
删除: with
删除: in Period II_D
删除: 56
删除: 75
删除: 69
删除: ,
删除: ing

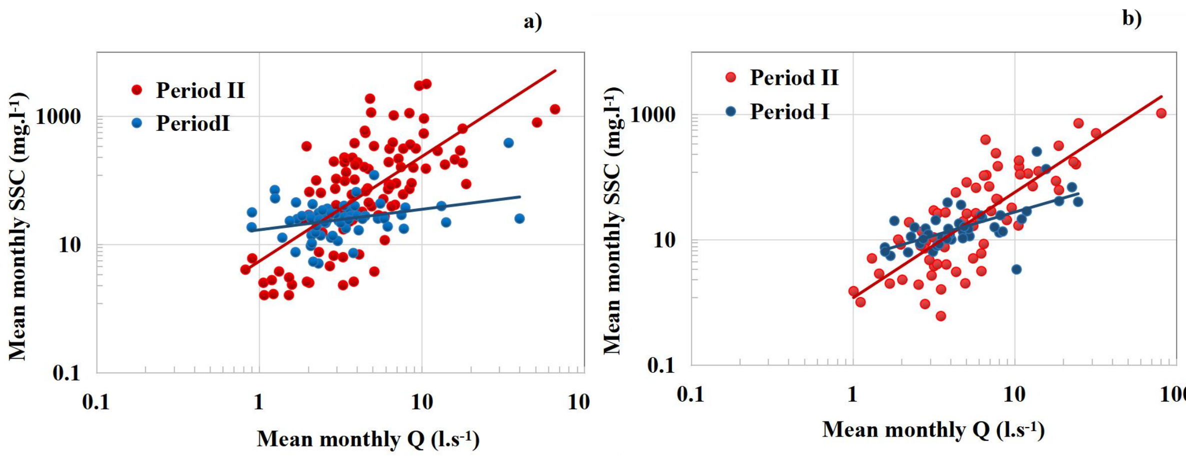

Figure 5 Sediment rating curves for a) the growing seasons and b) the dormant seasons in the two time periods. Each point represents a monthly mean observation.

Table 3 Parameter values for the coefficients of the SRC for different periods and seasons according to Equation (3).

Period	Coefficient		r^2
	a	***b***	
Period I_G	16.7	0.3	0.11
Period I_D	4.9	0.8	0.42
Period II_G	5.4	1.6	0.45
Period II_D	1.2	1.7	0.64

3.3.2 Relationship between coefficient *a* and *b*

The changing steepness of a fitted SRC does not necessarily imply a change in the sediment regime as the slopes of fitted SRC are sometimes affected by catchment size or the distribution of samples (Asselman, 2000). To minimize possible interference of other factors in identifying variations or shifts of the SRC, we investigated the relationship between coefficients *a* and *b* of the SRC. Figure 6 shows the coefficients log *(a)* plotted against *b* for the four investigated time frames. Interestingly, the data points of both Periods I and II, for the growing season are more concentrated in the lower right part of the graphs (Figure 6a). A different pattern of log (*a*) against *b* was

删除:
删除: **56**
删除: **one**
删除: **mean**
删除: **2**
删除: 2
删除: 2
删除: 0
删除: 75
删除: 38
删除: 3
删除: 17
删除: 69
删除: sometimes
删除: This technique was used by Asselman et al. (2000)
删除: 67
删除: displays
删除: Even though monthly averages were used for the sa
删除: in
删除: ,
删除: -lower
删除: area
删除: 7
删除: , although different sampling practices were used in
删除: whereasilstcauseda
删除: biased
设置格式: 非突出显示
删除: distribution of
删除: and

found for the dormant season (Figure 6b), i.e. the data points of Period I concentrated in the lower right area (blue points). But the points were more concentrated in the upper left area for Period II.

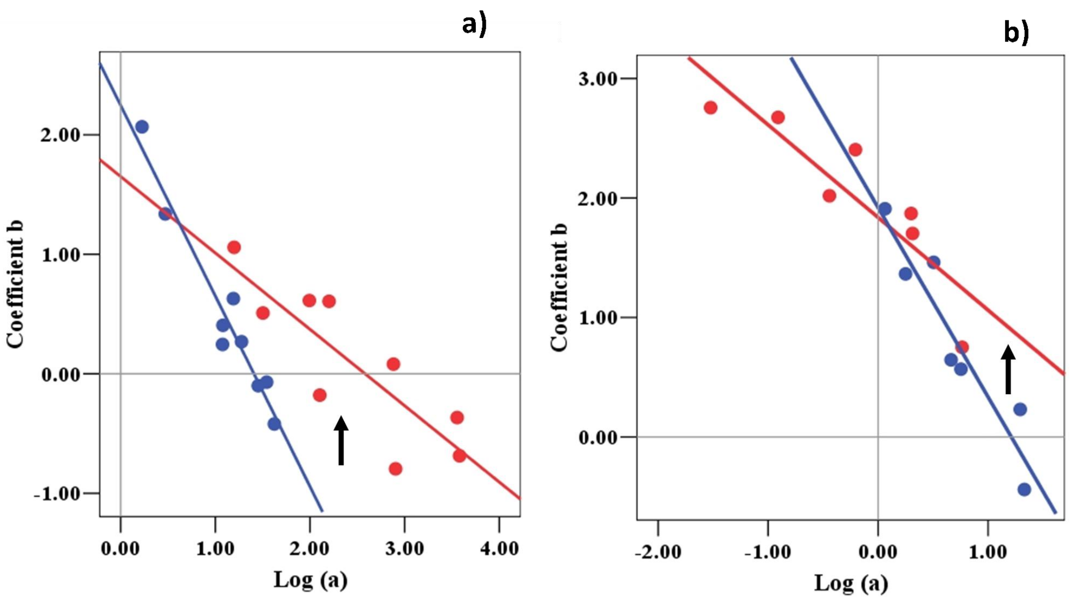

Figure 6 Relationship between coefficients *a* and *b* for a) growing season and b) dormant season of Period I (blue) and Period II (red), respectively. log (*a*) in x-axis represents the decadal logarithm. The arrows represent the shift of the sediment regime between Period I and Period II (see text below). All regressions are significant at $p<0.05$.

According to Asselman (2000), a shift of sediment regime means an alteration of either soil erodibility and/or erosive power of the river. In Figure 6, we found that the regression lines of Periods I to II are different. The intercepts of the regression lines are significantly different ($p<0.05$) for the growing seasons (Figure 6a). The slopes of the regression lines for Periods I and II were -1.60 and -0.94 in the growing season (Figure 6a), and -1.58 and -0.80 in the dormant season, respectively (Figure 6b). The upward shift of the line at log (*a*) larger than around 0.6 suggests that in Period II,

删除: in

删除: 7

删除: .

设置格式: 字体: 非倾斜

删除: Data

删除: is

删除: -lower

删除: . In contrast,

删除: ,

删除: b

删除: -upper

删除: whilst

删除: data of

删除: is more concentrated in the left-upper area

删除: , which is especially true during the dormant season

删除:

删除: **67**

设置格式: 字体: 小四

删除: **Throughout the manuscript, The**

设置格式: 字体: 倾斜

删除: **log10 (x)**

删除: **, and the rest of the main text has the same mean**

删除: **shifted**

删除: **upward**

删除: **to a certain degree (*i.e.* an alteration of either soi**

设置格式: 字体: 倾斜

设置格式: 字体: （默认）Times New Roman, 小四, 加粗

设置格式: 字体: （默认）Times New Roman, 小四, 加粗

设置格式: 字体: （默认）Times New Roman, 小四, 加粗

删除: T

删除: Nevertheless, whathowever the distribution of the d

设置格式: 突出显示

删除: relations

删除: between

most of the sediment was transported at relatively high flow rates. Since climate change was not responsible for the increased hydrological regime (see section 3.1), we mainly attribute this shift to the increase in hydrological connectivity, such as flow path density and flow length, and a change in land use and land cover statistics.

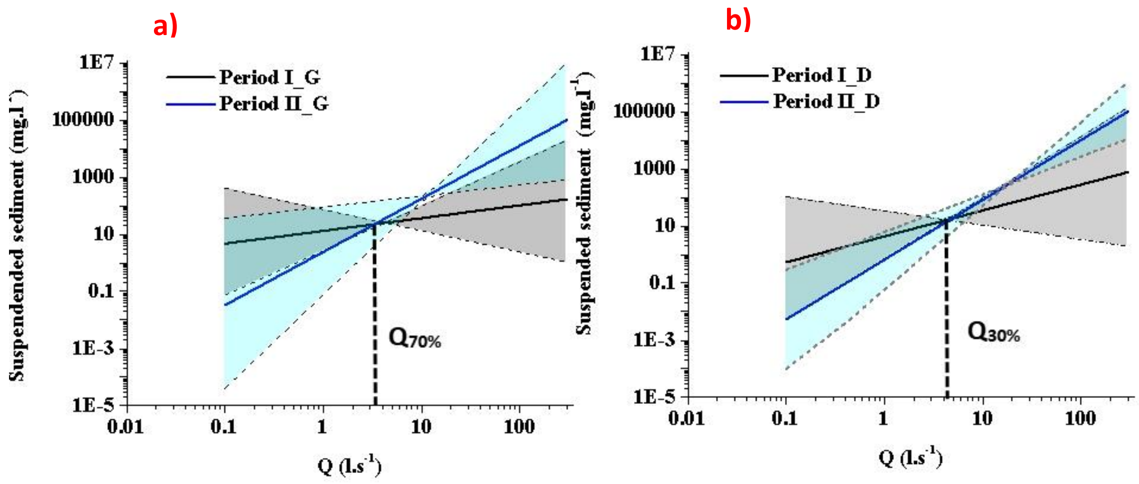

Figure 7 Theoretical sediment rating curves (tSRC) for the growing seasons (a) and the dormant seasons (b) of Period I and II. Solid lines denote the 50 percentile of the tSRC for each period (i.e. $tSRC_{50\%}$). The grey area denotes the range of the predicted tSRC composed of 5 and 95 percentiles (i.e. $tSRC_{5\%}$ and $tSRC_{95\%}$). $Q_{30\%}$ and $Q_{70\%}$ represent the flow conditions of 3.9 l·s^{-1} and 2.0 l·s^{-1}, respectively.

Figure 7 displays the theoretical sediment rating curves (tSRC) with their uncertainties for the different periods and seasons. At a given *Q* higher than approximately *$Q_{70\%}$*, sediment concentrations in Period II_G were higher than those in Period I_G (Figure 7a), whereas for flow rates below this value sediment concentrations were not different. The increased sediment concentrations in Period II_G are in line with the observations of the sediment load of Period II_G (6.3±32.5 t per month) which is largely enhanced compared to that of Period I_G (0.4±0.9 ton

删除: <sp>
删除: **8**
设置格式: 字体: 非倾斜
设置格式: 字体: 非倾斜
删除:
设置格式: 字体: 倾斜
设置格式: 字体: 倾斜
设置格式: 字体: 非倾斜
设置格式: 字体: 非倾斜
删除: 8
删除: , to allow for directly discriminating the change in
删除: ANCOVA suggests that the derived $tSRC_{50\%}$ were
设置格式: 字体: 倾斜
设置格式: 字体: 倾斜
删除: considerably
删除: (Figure 8a)
删除: whilst
删除: at the rest of the
删除: ,sediment concentrations were not different
删除: are
删除: as the gray area of the two tSRCs
删除: is
删除: general
删除: transport
删除: regime
删除: finding at most of timeis
删除: supported
删除: by the significant change in
删除: 19.9
删除: on
删除: which was significantly
删除: greatly higher
删除: (*p*<=0.056, t-test) than
删除: 6.3±19.9 ton per month during Period II_G compa

per month), see Table 4. Sediment concentrations were less different between the dormant seasons of Period I and Period II at flow rates lower than $Q_{30\%}$ (Figure 7b), which is also reflected by the insignificant (p>0.05) difference in sediment loads between Period I_D and Period II_D (being 0.6±1.1 and 3.2±14.0 t per month, respectively). However, an ANCOVA suggests that the derived tSRC$_{50\%}$ were significantly different (p<0.05) between the two periods, both in the growing seasons and dormant seasons. This enables us to estimate LUCC_effect and Parcel_effect according to the derived tSRCs.

Table 4 Monthly mean sediment loads and associated standard deviations of different periods

Period	Growing season (t month^{-1})	Dormant season (t month^{-1})
Period_I	0.4±0.9	0.6±1.1
Period_II	6.3±32.5	3.2±14.0

Note: Estimates based on equation (2)

3.4 Parcel_effect versus LUCC_effect

Figure 8 demonstrates the dynamic contributions of land structure (Parcel_effect) and LUCC changes (LUCC_effect) on sediment concentrations with increasing flow. Land structure change and the increase in cropland as well as a shift to crops with high risk of erosion explain the increase in sediment yield. However, the extent of their contributions to this increase differ. Generally, with higher flow rates, the contribution of the LUCC_effect gradually decreased, whilst the contribution of the Parcel_effect increased. The Parcel_effect accounted for more than 50% of the Total_effect after the flow rate exceeded 20 l s^{-1}approximately (i.e. $Q_{2\%}$) (Figure 8), exhibiting a dominant role in sediment production. This opposite trend of the relative contributions of the LUCC_effect and the Parcel_effect suggests that, even though land structure change

删除: ,
删除: ,
删除: (
删除: S
设置格式: 非突出显示
删除:),although there might be a certain degree of bias
删除: concentration
删除: regime
删除: s
删除: s
删除: in the dormant season of Period II was considerabl
设置格式: 字体: 倾斜, 非突出显示
设置格式: 非突出显示
删除: could be
设置格式: 字体: 倾斜, 非突出显示
设置格式: 非突出显示
删除: The stringent requirement on flow condition to de
设置格式: 字体: 倾斜, 非突出显示
设置格式: 非突出显示
删除: Observation of sediment loads offor
删除: I
删除: (5.4±18.3ton per month)
删除: higher thanthat of
删除: on
删除: (1.3±3.9 ton per month)
删除: butwithout stastically difference (p=0.07)
删除: although the degree of their difference varied with
删除: both
设置格式: 行距: 单倍行距
删除: **Statistic of**
删除: **monthly mean**
删除: **for**
删除: **on**
删除: ·

and LUCC both have unbeneficial effects on erosion control, their hydrological consequences may be different. Land structure change probably explaines much of the variation of sediment load at high flow conditions.

Unlike the situation during high flow rates, the Total_effect showed an almost zero value at flow rates less than approximately 2 l·s^{-1} (i.e. $Q_{70\%}$), suggesting no difference in sediment load between Periods I and II at low flow conditions. The increase in sediment concentration at flow rates of 2 l.s^{-1} up to around 20 l.s^{-1} seemed to be mainly caused by the changes in LUCC of Period II, as the contribution from the LUCC_effect was consistently higher than that of the Parcel_effect.

One may note that forest land cover increased considerably from Period I to Period II. We hypothesize that even though a beneficial effect of forest increase (up to a total of 11% of the catchment) may have appeared in Period II, it was easily offset by the negative effect of crop land changes, particularly the increase in row crops that are in general at a high risk of erosion. This contributed substantially to sediment yield compared with other land uses and other crop types (Kijowska‑Strugała et al., 2018).

删除: an increase in cropland

删除: ,

删除: with l

删除: ing

设置格式: 字体: 非倾斜

设置格式: 字体: 非倾斜

设置格式: 下划线

删除: (Figure 89)

删除: load

删除: ,

设置格式: 非上标/ 下标

设置格式: 字体: 非倾斜

删除: ,

删除: mainly

删除: due to

删除: the increase in the cropland area

删除: It, however, did not show an influential role in erosion control.

删除: accounting for

删除: around

删除: erosive

删除: ,

删除: which

删除: usually

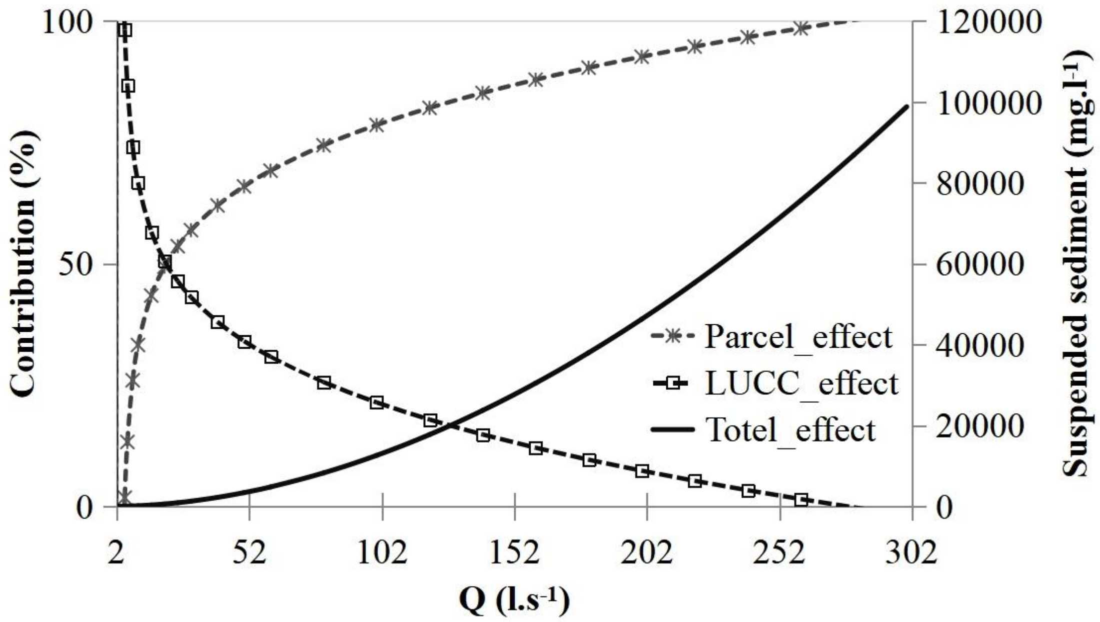

Figure 8 Contribution of Parcel_effect and LUCC_effect to the Total_effect across various flow rates. Total_effect (Equation 4) is displayed in terms of suspended sediment concentration. Parcel_effect and LUCC_effect was estimated by Equations (5) and (6), respectively; their contribution to the Total_effect was estimated by Equations (7) and (8), respectively.

4. Discussion

The industrial intensification of agriculture implemented during the last 70 years has raised considerable concerns regarding erosion and sediment loading of rivers (e.g. Bakker et al., 2008; Chevigny et al., 2014). However, with global climate warming, the different contributions of LUCC, land policy adjustments (i.e. land structure changes), and climate change affecting sediment load remain not well understood. This paper aims at evaluating the relative roles of climate change, LUCC, and land structure changes for sediment production, particularly at different flow rates.

4.1 Change in sediment load between two time periods

删除: <sp><sp>

删除: 89

删除: 3

删除: 4

删除: 5

删除: 6

删除: 7

删除:

删除: I

删除: in

删除: such as land consolidation

删除: are

删除: consolidation

删除: in

删除: varying

删除:

删除: This paper aims at evaluating the relative roles of climate change, land use and land cover changesLUCC, and land consolidation in sediment production, particularly forat varying flow rates.

We found that the sediment load increased almost six fold from Period I to Period II. This finding is supported by estimates of the management factor (C-Factor) and the slope and slope length factor (SL-Factor) of the RUSLE for Period I and Period II (Fiener et al., 2020). The C-Factor integrates changes in land use and crop statistics, thus it directly corresponds to changes of LUCC. The SL-Factor integrates parcel slopes and parcel sizes. Considering that the slopes in the HOAL did not change between the two periods, the SL-Factor may be used as direct indicator for changes in land structure. While the mean C-Factor of the HOAL catchment increased from 0.16 in Period I to 0.33 in Period II, the SL-Factor increased from 0.76 to 0.96. Added together, the changed values for these two factors increased the theoretical soil loss within the catchment by over 150%. This value is smaller than the changes observed, however it should be noted, that the RUSLE has not been designed to account for sediment loads of catchments but to estimate field scale soil loss within catchments. This may explain the observed differences to a certain extent.

4.2 Potential interference of different sampling methods

Due to technical advancement over the long investigation period, different sampling methods, i.e. grab sampling and automatic equal-discharge-increment sampling, were used in this study for Periods I and II. This may affect both rating curve estimation and sediment load estimation (Harmel et al., 2010; Thomas, 1988).

To test a potential influence that may result from the different sampling frequencies in the two periods, we resampled the data set of Period II. We randomly selected

删除:
删除: substantially
删除: II
删除: which
删除: are
删除: the calculation
删除: . For the methodology to calculate the different fact
删除:
删除: (
删除: Because
删除: with
删除: over
删除: over
删除: f
删除: Taken together
删除: One may note that
删除:
删除: a
设置格式: 字体: 非倾斜
删除: filed
删除: (EWDI) field
删除: our
删除: ., respectively, which
删除: which
删除: will
删除: was commonly believed to greatly affecting
删除: .
删除: (Thomas, 1988; Harmel et al., 2010;Groten and
删除: (
删除:).
删除:
删除:
删除: investigated the impacts of grab sampling, manuall
删除: (

repeated subsamples (n=10) of the *Q-C* observations of Period II with equal sample size to that of Period I. With each of the resampled datasets, we calculated SRCs. Combined with the flow data, the derived 10 SRCs were then used to calculate a mean annual sediment load. Comparing the mean annual sediment load from the resampling (62.4±10.2 t· yr^{-1}) to that of the original data set (60.0±140.0 t· yr^{-1}) resulted in an insignificant difference, suggesting that the different sampling strategies of Periods I and II did not affect the results.

Further support to the validity of our results is provided by Groten and Johnson (2019), who suggested that for sediment with very fine textural composition, the bias of different sampling strategies might be small. In our study catchment, the topsoil of the catchment is very fine textured consisting of 75% silty loam, 20% silty clay loam, and 5% silt according to the USDA soil classification (Picciafuoco et al., 2019).

4.3 Dynamic relevance of land consolidation in controlling sediment load

Climate change in terms of both monthly erosivity density (*ED*) and precipitation (*P*) was not responsible for the increase in sediment load, instead it could be explained by LUCC and land structure changes. This finding is particularly important in regions, where a strong intensification of agricultural management took place during the last decades. The relative contributions of LUCC and land structure changes varied with streamflow. For flow conditions below around 5 l.s^{-1}(i.e. Q_{20}%), land structure change had no apparent adverse effect on erosion, but with increasing flow, the contribution

设置格式: 字体: 倾斜, 非突出显示
设置格式: 非突出显示
设置格式: 字体: 倾斜, 非突出显示
设置格式: 非突出显示
删除: ’
删除: ’
删除: exercise
设置格式: 非突出显示
设置格式: 非突出显示
删除: indicated,
删除: ,
删除: se
删除: es
删除: ay
删除: between different sampling methods is smaller
删除: there is less of a difference among samples collecte
删除: investigated
删除: according to the USDA soil classification,
删除: constituted
删除: The extremlyfined soil texture has actually enabled
设置格式: 突出显示
设置格式: 字体: 加粗, 倾斜, 突出显示
设置格式: 突出显示
设置格式: 字体: 加粗, 倾斜, 突出显示
设置格式: 突出显示
设置格式: 突出显示
设置格式: 突出显示
设置格式: 上标
设置格式: 突出显示
删除: this effect
删除: can
删除: land cover
删除: consolidation
删除: and their relative contributions varied with streamflow

to sediment load increased continuously, leading to a dominant role at high flow rates. This finding is partially in line with David et al. (2014) and Cantreul et al. (2020). They reported that landscape structure was less important for soil erosion than LUCC during normal flow conditions. However, they did not investigate whether the effect of landscape structure showed a dynamic behavior with increasing flow. In contrast, the LUCC_effect, i.e. the increase of crops with high erosion risk and the change in land use, continuously affected sediment load with gradually decreasing importance at high flow conditions. Similar results were reported by Vaughan et al. (2017), who showed that sediment concentration at low and median flow conditions was considerably associated with a change in catchment characteristics, primarily land use and land cover. Although the role of LUCC was dominating for flow conditions less than Q_{20}%, it's contribution to the total annual sediment load was small. More than 75% of the total sediment load was transported during a small number of events (25 events in Period I, 8 events in Period II) and all events had flow rates above 15 l.s^{-1}(approximately at $Q_{13\%}$ in Period I or $Q_{4\%}$ in Period II, respectively), which underlines the importance of land structure for sediment loading.

The dynamic relevance of LUCC and land structure changes in sediment production is associated with the processes and mechanisms controlling overland flow as a transporting agent for sediment (e.g. Sun et al., 2013; El Kateb et al., 2013; Nearing et al., 2017; Silasari et al., 2017; Kijowska - Strugała et al., 2018). A change in types of land use and used crops (LUCC) implies alterations of surface characteristics, such as above ground structure morphology, litter cover, organic matter components, root

删除: extremely

删除: duringat most normal flow conditions

删除: land use and land cover

删除: for

删除: and extreme

删除: have been

删除: effect

删除: land use changes

删除: below

设置格式: 字体: 非倾斜

删除: at

设置格式: 字体: 倾斜

删除: and

设置格式: 字体: 倾斜

删除: l

删除: .

删除:

删除: is

删除: s

删除: vegetation

删除: consolidation

删除: behavior

删除: loading

删除: isare

删除: ir

删除: of vegetation

删除: Kijowska - Strugała et al., 2018;

删除: land cover

network (Gyssels et al., 2005; Wei et al., 2007; Moghadam et al., 2015; Patin et al., 2018) and soil properties (Costa et al., 2003; Moghadam et al., 2015). These properties influence the protective role of vegetation in soil detachment, the flow capacity to transport sediment particles, and runoff flow paths to the stream channels (Van Rompaey et al., 2002; Lana-Renault et al., 2011; Sun et al., 2018). The protective effects tend not to linearly increase with increasing surface runoff. Accelerated discharge and stronger scouring effects of upslope discharge might impair the protective role of vegetation (e.g. Zhang et al., 2011; Santos et al.,2017; Bagagiolo et al., 2018; Yao et al., 2018; Wang et al., 2019). Vegetation usually exhibits a smaller interception capability at high rainfall intensity, resulting in an enhanced splash erosion and availability of mobile soil particles (Cayuela et al., 2018; Magliano. et al., 2019; Nytch et al., 2019). However, the decreasing contribution of the LUCC_effect does not directly imply an absolute decrease of the magnitude of the LUCC_effect. The absolute change in sediment concentration resulting from LUCC reveals an increasing trend as flow rates increase. Thus, the contribution of the LUCC_effect stands for the relevance of LUCC in erosion control compared to the change due to land structure. The magnitude of the LUCC_effect probably depends mainly on where within the catchment the LUCC is changed and how the proportional area of various land uses changes. We will address this topic in future analyses.

Unlike land cover and land use change, landscape structure is usually combined with other catchment properties, such as slope characteristics and soil properties (Gascuel-Odoux et al., 2011) and additional erosion and transport factors (Verstraeten

删除: river

删除: Nevertheless, t

删除: do

设置格式: 字体: 非倾斜

删除: Yao et al., 2018;

删除: capacity

删除: SSC

删除: s

删除: consolidation

删除: land cover

删除: was

删除: replaced

删除: d

删除: issue

et al., 2000). These factors exert a more complicated influence on erosion. For example, the effect of landscape structure on soil erosion may be identified on moderate slopes, while on steep slopes it may be concealed by on-site severe soil erosion (Chevigny et al., 2014). However, the key process for erosion control is the fact that landscape elements and their structural position (i.e. parcel structure, field boundaries, hedges and similar) alter hydrological connectivity between land and water. This is particularly true when the land cover on both sides of boundaries is different (Van Oost et al., 2000). Reducing parcel size and heterogeneity increases hydrological connectivity significantly and results in a substantial off-site damage effect, irrespective of on-site erosion of the investigated land use (Boardman et al., 2018; Devátý et al., 2019). During low and median flow conditions, surface runoff and sediment may arrive to a lesser extent at field boundaries due to efficient interception effects of the vegetation cover. This may explain the identified dynamic relevance of land structure change in sediment load found here.

5 Conclusions

Climate change, land use and land cover change, and other human-associated activities are widely regarded as potential agents driving hydrological change. Understanding the relevance of each of these agents in the hydrological cycle is critical for implementing adaptive catchment management measures and addressing climate change. Although very significant climate change influences in the last decades have been identified for certain components of the hydrological cycle we

删除: ,

删除: ing

删除: control

删除: herein

删除: Our findings are also supported by the calculation of the management factor (C-Factor) and the slope and slope length factor (SL-Factor) of the RUSLE for Period I and Period II. While the mean C-Factor of the HOAL catchment increased from 0.16 during Period I to 0.33 for Period II, the SL factor increased from 0.76 to 0.96 from Period I to Period I. Taken together, the changed values for these two factors increase the theoretical soil loss within the catchment by over150%. This is smaller than the changes observed, however it should be noted that the RUSLE has not been designed to account for sediment loads of catchments but to estimate field scale soil loss within catchments. This may explain the observed differences to a certain extent.

删除: factors

删除: For some hydrological cycle components,

删除: some

删除: components (e.g. Haslinger et al., 2019; Duethmann and Blöschl, 2018).,However, found that climate change expressed in changes in rainfall erosivity and precipitation cannot explain the increased sediment production between 1946-1954 and 2002-2017 in the investigated catchment. Instead, both LUCC and land structure change played important, dynamic roles in erosion and sediment production.

The relevance of land use and land cover change versus land structure change varied dynamically with changing flow conditions. The reduction in parcel density undoubtedly increased sediment load, particularly at higher flows due to the decreased capacity of trapping sediment particles between parcels and increasing flow lengths inside parcels. Unfavorable land use or land cover change increased sediment load at most flow conditions, although the relevance of this process decreased at high or very high flow rates. Therefore, when addressing soil conservation measures at the catchment scale, the distribution of fields, land structure, and vegetation cover should be simultaneously considered. Such a strategy would be conducive to deal with the risk of soil erosions at different flow rates. Land use policy adjustments resulting from technological development have been vital to deal with food security issues in the past. However, now we experience the negative influence of these adjustments on the hydrological cycle. Therefore, rather than focusing on climate change solely, we need to pay increased attention to anthropic management activities to counteract their negative impact on hydrological change effectively.

删除: land cover

删除: consolidation

删除: controlling

删除: Still, t

删除: consolidation

删除: cu

删除: increases

删除: soil erosion risk

删除: Meanwhile,

删除: u

删除: will

删除: would decreasediminishes

删除: s

删除: Meanwhile, unfavorable land use or land cover change will increase sediment load at most normal flow conditions, although the relevance of this process would decrease at high or very high flow rates

删除: ing

删除: Our findings are particularly important in regions, where a strong intensification of agricultural management took place during the last decades.

删除: have to

Author contributions

Shengping Wang has led the data analysis, drafted the manuscript, and revised the manuscript; Peter Strauss was responsible for the project design, oversaw the whole analysis, and conducted manuscript revision as the project leader; Carmen Krammer was responsible for data collection and data preparation; Elmar Schmaltz has contributed to figure drawing and manuscript revision; Borbala Szeles has helped with data analysis and manuscript revision; Kepeng Song and Yifan Li helped with data processing; and Günter Blöschl oversaw and critically reflected on the manuscript writing as the senior scientist.

删除: Dr.

删除:

删除: Dr.

删除: Dr.

删除: Dr.

删除: Dr.

删除: to revise the

删除: ,

删除: Mr.

删除: Mr.

删除: to part of

删除: Prof.

删除: revision

Competing interests

The authors declare that they have no conflict of interest.

Disclaimer

Publisher's note: Copernicus Publications remains neutral with regard to jurisdictional claims in published maps and institutional affiliations.

Acknowledgements

This work is financially supported by the SHUI project (Soil Hydrology research platform underpinning innovation to manage water scarcity in European and Chinese cropping systems) within the Horizon 2020 Research and Innovation Action of the European Community (No. 773903), the Austrian Science Funds (FWF), project W1219-N28, and the TU Wien Risk network.

References

Asselman, N. E. M. Fitting and interpretation of sediment rating curves, Journal of Hydrology, 234(3-4), 228-248 https://doi.org/10.1016/S0022-1694(00)00253-5, 2000.

Awal, R., Sapkota, P., Chitrakar, S., Thapa, B. S., Neopane, H. P., & Thapa, B.: A General Review on Methods of Sediment Sampling and Mineral Content Analysis, Journal of Physics:

删除: 2000.

删除: .

删除: Journal of HydrologyOH

删除: .

设置格式: 字体: 五号

设置格式: 字体: 五号

设置格式: 字体: （默认）Times New Roman, 无下划线

设置格式: 正文, 左, 段落间距段前: 0.5 行, 行距: 多倍行距 1.25 字行

设置格式: 字体: （默认）Times New Roman, 无下划线

删除: .

设置格式: 字体: （默认）Times New Roman, 无下划线

Conference Series, 1266(1), https://doi.org/10.1088/1742-6596/1266/1/012005, 2019

Bagagiolo, G., Biddoccu, M., Rabino, D., Cavallo, E.: Effects of rows arrangement, soil management, and rainfall characteristics on water and soil losses in Italian sloping vineyards, Environmental Research, 166, 690-704, 2018

Bakker, M., Govers, G., van Doorn, A., Quetier, F., Chouvardas, D., Rounsevell, M.: The response of soil erosion and sediment export to land-use change in four areas of Europe: The importance of landscape pattern, Geomorphology, 98, 213-226, 2008.

Baudry, J. and Merriam, H.G.: Connectivity in landscape ecology, in: Proc. 2nd Intern. Semin. of IALE, Muenster 1987. Muensterische Geographische Arbeiten 29, 23-28, 1988

Bellin, N., Vanacker, V., De Baets, S.: Anthropogenic and climatic impact on Holocene sediment dynamicsin SE Spain: A review, Quaternary International, 308-309,112-129, 2013

Bochet, E., Poesen, J., Rubio, J.L.: Runoff and soil loss under individual plants of a semi-arid Mediterranean shrubland: influence of plant morphology and rainfall intensity, Earth Surf. Process. Landforms, 31, 536-549, 2006.

Bouma, J., Varallyay, G., Batjes, N.H.: Principal land use changes anticipated in Europe. Agr. Ecosyst. Environ., 67 (2-3), 103-119, 1998.

Blöschl, G., Blaschke, A. P., Broer, M., Bucher, C., Carr, G., Chen, X., Eder, A., Exner-Kittridge, M., Farnleitner, A., Flores-Orozco, A., Haas, P., Hogan, P., KazemiAmiri, A., Oismüller, M., Parajka, J., Silasari, R., Stadler, P., Strauss, P., Vreugdenhil, M., Wagner, W., and Zessner, M.: The Hydrological Open Air Laboratory (HOAL) in Petzenkirchen: a hypothesis-driven observatory, Hydrol. Earth Syst. Sci., 20, 227-255, doi:10.5194/hess-20-227-2016, 2016.

Cantreul, V., Pineux, N., Swerts, G., Bielders, C., Degré, A.: Performance of the LandSoil expert-based model to map erosion and sedimentation: application to a cultivated catchment in central Belgium,Earth Surf. Process. Landforms,DOI: 10.1002/esp.4808, 2020

Cayuela, C., Llorens, P., Sanchez-Costa, E.,Levia, D.F， Latron, J.:Effect of biotic and abioticfactors on inter- and intra-eventvariability in stemflow rates in oak and pine stands in a Mediterraneanmountain area, Journal of Hydrology, 560: 396-406, 2018.

Chevigny, E., Quiquerez, A., Petit, C., Curmi, P.:Lithology, landscape structure and management practice changes: Key factors patterning vineyard soil erosion at metre-scale spatial resolution, CATENA, 121, 354-364, 2014.

Costa, M.H., Botta, A., Cardille, J.A.: Effects of large scale changes in land cover on the discharge

删除: .
设置格式: 字体: （默认）Times New Roman, 无下划线
设置格式: 字体: （默认）Times New Roman, 无下划线
设置格式: 字体: （默认）Times New Roman
设置格式: 字体: （默认）Times New Roman
删除: 2018.
删除: .
删除: :
删除: .
删除: 2008.
删除: .
删除: :
删除: .
删除: 1988.
删除: .
设置格式: 字体: 五号, 无下划线, 字体颜色: 自动设置
删除: :
设置格式: 字体: 五号, 无下划线, 字体颜色: 自动设置
删除: .
设置格式: 字体: 五号, 无下划线, 字体颜色: 自动设置
设置格式: 德语(奥地利)
设置格式: 字体: 五号, 无下划线, 字体颜色: 自动设置
删除: 2013.
删除: .
删除: :
删除: .
删除: 2006.
删除: .
删除: .
删除: .
删除: 1998.
删除: :
删除: .
删除: 2016.

of the Tocantins River, Southeastern Amazonia, Journal of Hydrology, 283, 206-217, 2003.

David, M., Follain, S., Ciampalini, R., Le Bissonnais, Y., Couturier, A., Walter, C.:Simulation of medium-term soil redistributions for different land use and landscape design scenarios within a vineyard landscape in Mediterranean France, Geomorphology, 214, 10-21, 2014.

Desilets, S.L.E., Nijssen, B., Ekwurzel, B., Ferre, T.P.A.: Post-wildfire changes in suspended sediment rating curves: Sabino Canyon, Arizona,Hydrol. Process., 21,1413-1423, 2007

Devátý, J., Dostál, T., Hösl, R., Krása, J., Strauss, P.:Effects of historical land use and land pattern changes on soil erosion - Case studies from Lower Austria and Central Bohemia, Land Use Policy, 82, 674-685,https://doi.org/10.1016/j.landusepol.2018.11.058, 2019

Duethmann, D., and Blöschl, G.:Why has catchment evaporation increased in the past 40 years? A data-based study in Austria. Hydrology and Earth System Sciences, 22, 5143-5158,https://doi.org/10.5194/hess-22-5143-2018, 2018.

Eder, A., Exner-Kittridge, M., Strauss, P., Blöschl, G.:Re-suspension of bed sediment in a small stream – results from two flushing experiments,Hydrology and Earth System Sciences, 18, 1043–1052, 2014

El Kateb, H., Zhang, H.F., Zhang, P.C., Mosandl, R.: Soil erosion and surface runoff on different vegetation covers and slope gradients: A field experiment in Southern Shaanxi Province, China, CATENA, 105,1-10, 2013

Fan, X., Shi, C., Zhou, Y., Shao, W.: Sediment rating curves in the Ningxia-Inner Mongolia reaches of the upper Yellow River and their implications, Quaternary International, 282, 152-162,https://doi.org/10.1016/j.quaint.2012.04.044, 2012

Fiener, P., Dostal, T., Krasa, J., Schmaltz, E., Strauss, P., and Wilken, F.: Operational USLE-Based Modelling of Soil Erosion in Czech Republic, Austria, and Bavaria – Differences in Model Adaptation, Parametrization, and Data Availability, Applied Sciences, 10, 3647, 1-18, Doi:10.3390/app10103647, 2020.

García-Ruiz, J. M.:The effects of land uses on soil erosion in Spain?: A review, CATENA, 81(1), 1-11, https://doi.org/10.1016/j.catena.2010.01.001, 2010.

Gascuel-Odoux, C., Aurousseau, P., Doray, T., Squividant, H., Macary, F., Uny, D., Grimaldi, C.:Incorporating landscape features to obtain an object-oriented landscape drainage network representing the connectivity of surface flow pathways over rural catchments, Hydrological Processes, 25(23), 3625-3636, 2011.

删除: .
删除: J. Hydrol
删除: .
删除: 2014.
删除: .
删除: :
删除: , 2007.
删除: .
删除: .
删除: 2019.
删除: .
删除: (January)
删除: .
设置格式: 字体: 五号
删除: 2018.
设置格式: 字体: （默认）Times New Roman, 五号,
设置格式: 字体: （默认）Times New Roman, 五号,
设置格式: 字体: （默认）Times New Roman, （中文
设置格式: 字体: (默认)Times New Roman, (中文)T
设置格式: 正文, 段落间距段前: 0.5 行, 行距: 多倍行
设置格式: 字体: (默认)Times New Roman, (中文)T
设置格式: 默认段落字体, 字体: (默认)Times New R
设置格式: 字体: (默认)Times New Roman, (中文)T
设置格式: 字体: 五号, 德语(奥地利)
删除: 2013.
删除: .
删除: :
删除: .
删除: 2012.
删除: .
删除: .
设置格式: 字体: 五号
设置格式: 字体: （默认）Times New Roman, 五号,
设置格式: 正文, 左, 段落间距段前: 0.5 行, 行距: 多

Groten, J. T., & Johnson, G. D.:Comparability of river suspended-sediment sampling and laboratoryanalysismethods,Scientific Investigations Report, 1–23, 2018.

Guzman, C. D., Tilahun, S. A., Zegeye, A. D., Steenhuis, T. S.: Suspended sediment concentration-discharge relationships in the (sub-) humid Ethiopian highlands, Hydrology and Earth System Sciences, 17(3), 1067-1077,https://doi.org/10.5194/hess-17-1067-2013, 2013.

Gyssels, G., Poesen, J., Bochet, E., Li, Y.:Impact of plant roots on the resistance of soils to erosion by water: a review, Prog. Phys. Geogr., 29, 189-217, 2005.

Harmel, R. D., Slade, R. M., & Haney, R. L.: Impact of Sampling Techniques on Measured Stormwater Quality Data for Small Streams, Journal of Environmental Quality, 39(5), 1734–1742,https://doi.org/10.2134/jeq2009.0498, 2010.

Haslinger, K., Hofstätter, M., Kroisleitner, C., Schöner, W., Laaha, G., Holawe, F., &Blöschl, G. :Disentangling Drivers of Meteorological Droughts in the European Greater Alpine Region During the Last Two Centuries, Journal of Geophysical Research: Atmospheres, 124(23), 12404–12425. https://doi.org/10.1029/2018JD029527, 2019.

Hou, J., Zhu, H., Fu, B., Lu, Y., Zhou, J.:Functional traits explain seasonal variation effects of plant communities on soil erosion in semiarid grasslands in the Loess Plateau of China, CATENA, 194, 104743,https://doi.org/10.1016/j.catena.2020.104743, 2020.

Hu, B., Wang, H., Yang, Z., & Sun, X.:Temporal and spatial variations of sediment rating curves in the Changjiang (Yangtze River) basin and their implications,Quaternary International, 230(1–2), 34–43,https://doi.org/10.1016/j.quaint.2009.08.018, 2011.

IUSS Working Group WRB, World Reference Base for Soil Resources 2014, update 2015International soil classification system for naming soils and creating legends for soil maps, World Soil Resources Reports No. 106. FAO, Rome, 2015.

Kelly, C.N., Mc Guire, K.J., Miniat, C.F., Vose, J.M.: Streamflow response to increasing precipitation extremes altered by forest management. Geophys. Res. Lett. 43(8), 3727–3736,https://doi.org/10.1002/2016GL068058, 2016.

Khaledian, H., Faghih, H., Amini, A.: Classifications of runoff and sediment data to improve the rating curve method. Journal of Agricultural Engineering, 48(3), 147-153,https://doi.org/10.4081/jae.2017.641, 2017.

Kijowska‐Strugata, M., Bucała‐Hrabia, A., Demczuk, P.: Long-term impact of land use changes on soil erosion in an agricultural catchment (in the Western Polish Carpathians), Land

Degrad. Dev., 29,1871-1884, 2018.

Korkanç, S. Y.: Effects of the land use/cover on the surface runoff and soil loss in the Niğde-Akkaya Dam Watershed, Turkey, CATENA, 163:233–243,https://doi.org/10.1016/j.catena.2017.12.023, 2018.

Kottek, M., Grieser J., Beck, C., Rudolf, B., Rubel, F.: World Map of the Köppen-Geiger climate classification updated. Meteorol. Z., 15, 259-263. DOI: 10.1127/0941-2948/2006/0130, 2006.

Kundzewicz, Z.W. (Ed.): Changes in Flood Risk in Europe. IAHS Special Publication 10, 516 pp, 2012.

Lana-Renault, N., Latron, J., Karssenberg, D., Serrano-Muela, P., Reguees, D., Bierkens, M. F. P. :Differences in stream flow in relation to changes in land cover: A comparative study in two sub-Mediterranean mountain catchments, Journal of Hydrology, 411(3-4), 366-378, 2011.

Li, S., Bing, Z., Jin, G.:Spatially explicit mapping of soil conservation service in monetary units due to land use/cover change for the three gorges reservoir area, China. Remote Sensing, 11(4), 6-8,https://doi.org/10.3390/rs11040468, 2019.

Li, Y., Li, J.J., Are, K. S., Huang, Z.G.,Yu, H. Q., Zhang, Q.W.: Livestock grazing significantly accelerates soil erosion more than climate change in Qinghai-Tibet Plateau: Evidenced from 137Cs and 210Pbex measurements, Agriculture, Ecosystems & Environment, 285, doi:10.1016/j.agee.2019.106643, 2019.

Madarász, B., Jakab, G., Szalai, Z., Juhos, K., Kotroczó, Z., Tóth, A., Ladányi, M.: Long-term effects of conservation tillage on soil erosion in Central Europe: A random forest-based approach, Soil and Tillage Research, 209,https://doi.org/10.1016/j.still.2021.104959, 2021.

Madsen, H., Lawrence, D., Lang, M., Martinkova, M., Kjeldsen, T. R.: Review of trend analysis and climate change projections of extreme precipitation and floods in Europe, Journal of Hydrology, 519, 3634–3650,https://doi.org/10.1016/j.jhydrol.2014.11.003, 2014.

Magliano, Patricio N., Whitworth-Hulse, Juan, I., Florio, Eva L.,Aguirre，E.C.,Blanco, L.J.: Interception loss, throughfall and stemflow by Larreadivaricata: The role of rainfall characteristics and plant morphological attributes, Ecological Research, 34(6), 753-764, 2019.

Merriam, G.: Ecological processes in the time and space farmland mosaics,in: Changing Landscapes: An Ecological Perspective. 286 pp. Edited by S. Zonneveld and R.T.T. Forman, Springer-Verlag, New-York, pp. 121-126, 1990.

Moghadam, B., Jabarifar, M., Bagheri, M., Shahbazi, E.: Effects of land use change on soil splash

删除: :

删除: 2018.

删除: .

删除: .

设置格式: 默认段落字体，字体: (默认)Times New R

设置格式: 默认段落字体，字体: (默认)Times New R

删除: 2006

删除: , 2012.

设置格式: 字体: 五号，无下划线，字体颜色: 自动设

删除: 2019.

设置格式: 字体: 五号，无下划线，字体颜色: 自动设

删除: .

设置格式: 默认段落字体，字体: (默认)Times New R

设置格式: 默认段落字体，字体: (默认)Times New R

删除: 2019.

删除: .

删除: Lana-Renault, N., Latron, J., Karssenberg, D.,

删除: 2021.

删除: .

删除: .

删除: 2014.

删除: .

删除: .

设置格式: 字体: 五号，英语(美国)，(中文) 中文(简体)

删除: ,2019.

删除: .

删除: :

删除: 1990.

删除: .

删除: I

删除: 2015.

erosion in the semi-arid region of Iran Geoderma, 241-242, 210-220, 2015.

Moravcová, J., Koupilová, M., Pavlíček, T., Zemek, F., Kvítek, T., Pečenka, J.: Analysis of land consolidation projects and their impact on land use change, landscape structure, and agricultural land resource protection: case studies of Pilsen-South and Pilsen-North (Czech Republic), Landscape and Ecological Engineering, 13(1), 1-13 https://doi.org/10.1007/s11355-015-0286-y, 2017.

Mullan, Donall.: Soil erosion under the impacts of future climate change: Assessing the statistical significance of future changes and the potential on-site and off-site problems, CATENA, 109, 234-246, 2013.

Nampak, H., Pradhan, B., MojaddadiRizeei, H., Park, H. J.: Assessment of land cover and land use change impact on soil loss in a tropical catchment by using multitemporal SPOT-5 satellite images and Revised Universal Soil Loss Equation model, Land Degradation and Development, 29(10), 3440-3455 https://doi.org/10.1002/ldr.3112, 2018.

Nearing, M. A., Pruski, F. F., O'Neal, M. R.: Expected climate change impacts on soil erosion rates: A review, Journal of Soil and Water Conservation, 59 (1), 43-50, 2004.

Nearing, M. A., Xie, Y., Liu, B., Ye, Y.: Natural and anthropogenic rates of soil erosion, International Soil and Water Conservation Research, 5, 77-84 https://doi.org/10.1016/j.iswcr.2017.04.001, 2017.

Nytch, C. J., Melendez-Ackerman, E. J., Perez, M., Ortiz-Zayas J.R.: Rainfall interception by six urban trees in San Juan, Puerto Rico, Urban Ecosystems, 22(1), 103-115, 2019.

Palazon, L, Navas, A.: Land use sediment production response under different climatic conditions in an alpine–prealpine catchment, CATENA, 137, 244-255, 2016.

Patin, J., Mouche, E., Ribolzi, O., Sengtahevanghoung, O., Latsachak, K.O., Soulileuth, B., Chaplot, V., Valentin, C.: Effect of land use on interrill erosion in a montane catchment of Northern Laos: An analysis based on a pluri-annual runoff and soil loss database, Journal of Hydrology, 563, 480-494, 2018.

Perović, V., Jakšić, D., Jaramaz, D., Koković, N., Čakmak, D., Mitrović, M., Pavlović, P.:Spatio-temporal analysis of land use/land cover change and its effects on soil erosion (Case study in the Oplenac wine-producing area, Serbia), Environmental Monitoring and Assessment, 190 (11) https://doi.org/10.1007/s10661-018-7025-4, 2018.

Phillips, R. W., Spence, C., & Pomeroy, J. W.: Connectivity and runoff dynamics in heterogeneous

删除: .

删除: :

删除: 2017.

删除: .

删除: .

设置格式: 默认段落字体, 字体: (默认)Times New Ro

设置格式: 默认段落字体, 字体: (默认)Times New Ro

删除: 2013.

删除: .

删除: .

删除: :

删除: Mullan, D., Matthews, T., Vandaele, K., Barr, I. D.,

删除: 2018.

删除: .

删除: .

设置格式: 字体: 五号, 英语(美国), （中文）中文(简体)

删除: 2017.

删除: .

删除: .

删除: Nearing, M. A., Pruski, F. F., O'Neal, M. R. 2004.

设置格式: 字体: 五号, 无下划线, 字体颜色: 自动设置

删除: . 2019.

删除: .

删除: RBAN

删除: COSYSTEMS.

删除: :

删除: Ozsahin, E., Duru, U., Eroglu, I. 2018. Land use an

删除: 2016.

删除: .

删除: :

删除: 2018.

删除: .

删除: :

删除: 2018.

basins, Hydrological Processes, 25(19), 3061-3075 https://doi.org/10.1002/hyp.8123, 2011.

Picciafuoco, T., Morbidelli, R., Flammini, A., Saltalippi, C., Corradini, C., Strauss, P., &Blöschl, G.: A Pedotransfer Function for Field - Scale Saturated Hydraulic Conductivity of a Small Watershed, Vadose Zone Journal, 18(1), 1 - 15 https://doi.org/10.2136/vzj2019.02.0018, 2019

Prosdocimi, M., Cerdà, A., Tarolli, P.:Soil water erosion on Mediterranean vineyards: A review, CATENA, 141, 1-21 https://doi.org/10.1016/j.catena.2016.02.010, 2016.

Salesa, D., &Cerdà, A.:Soilerosion on mountain trails as a consequence of recreationalactivities. A comprehensivereview of the scientificliterature, Journal of Environmental Management, 271 https://doi.org/10.1016/j.jenvman.2020.110990, 2020.

Santos, J.C.N., de Andrade, E.M., Medeiros, P.H.A., Guerreiro, M.J.S., Palacio, H.A.D.: Effect of Rainfall Characteristics on Runoff and Water Erosion for Different Land Uses in a Tropical Semiarid Region, Water Resources Management, 31(1) 173-185, 2017.

Scholz, G., Quinton, J.N., Strauss, P.:Soil erosion from sugar beet in Central Europe in response to climate change induced seasonal precipitation variations CATENA, 72, 91 - 105 https://doi.org/10.1016/j.catena.2007.04.005, 2008.

Sharma, A., Tiwari, K. N., Bhadoria, P. B. S.: Effect of land use land cover change on soil erosion potential in an agricultural watershed, Environmental Monitoring and Assessment, 173(1-4), 789-801 https://doi.org/10.1007/s10661-010-1423-6, 2011.

Sheridan, G. J., Lane, P. N. J., Sherwin, C. B., Noske, P. J.: Post-fire changes in sediment rating curves in a wet Eucalyptus forest in SE Australia, Journal of Hydrology, 409(1-2), 183-195 https://doi.org/10.1016/j.jhydrol.2011.08.016, 2011.

Silasari, R., Parajka, J., Ressl, C., Strauss, P., and Blöschl. G.: Potential of time-lapse photography for identifying saturation area dynamics on agricultural hillslopes, Hydrological Processes, 31, 3610–3627, doi: 10.1002/hyp.11272, 2017.

Smakhtin, V.U.: Low flow hydrology: a review, Journal of Hydrology, 240 (3-4), 147-186, 2001.

Syvitski, J.P., Morehead, M.D., Bahr, D.B., Mulder, T.: Estimating fluvial sediment transport: the rating parameters, Water Resour. Res., 36 (9), 2747-2760, 2000.

Sun, D., Yang, H., Guan, D., Yang, M., Wu, J.B., Yuan, F.H., Jin, C.J., Wang, A.Z., Zhang, Y.S.:The effects of land use change on soil infiltration capacity in China: A meta-analysis, Science of the Total Environment, 626, 1394-1401, 2018.

删除: .

删除: :

删除: .

设置格式: 字体: 五号, 英语(美国), （中文）中文(简体)

设置格式: 字体: （默认）Times New Roman, 无下划线

设置格式: 正文, 左, 段落间距段前: 0.5 行, 行距: 多

设置格式: 字体: （默认）Times New Roman, 法语(法国)

设置格式: 字体: （默认）Times New Roman, 无下划线

设置格式: 字体: （默认）Times New Roman, 法语(法国)

设置格式: 字体: （默认）Times New Roman, 无下划线

设置格式: 字体: （默认）Times New Roman, 法语(法国)

设置格式: 字体: （默认）Times New Roman, 无下划线

设置格式: 字体: （默认）Times New Roman, 法语(法国)

设置格式: 字体: （默认）Times New Roman, 无下划线

设置格式: 字体: （默认）Times New Roman, 法语(法国)

设置格式: 字体: （默认）Times New Roman, 无下划线

设置格式: 字体: （默认）Times New Roman, 法语(法国)

设置格式: 字体: （默认）Times New Roman, 非倾斜,

设置格式: 字体: （默认）Times New Roman, 法语(法国)

设置格式: 字体: （默认）Times New Roman, 无下划线

设置格式: 字体: （默认）Times New Roman, 五号, 法

设置格式: 字体: （默认）Times New Roman, 法语(法国)

删除: 2016.

删除: .

删除: .

设置格式: 默认段落字体, 字体: （默认）Times New R

设置格式: 默认段落字体, 字体: （默认）Times New R

删除: 2020.

删除: .

删除: (June).

设置格式: 英语(美国)

删除: 2017.

删除: .

删除: :

Sun, P.C., Wu, Y.P., Wei, X.H., Sivakumar, B., Qiu, L.J., Mu, X.M., Chen, J., Gao, J.E.: Quantifying the contributions of climate variation, land use change, and engineering measures for dramatic reduction in streamflow and sediment in a typical loess watershed, China, Ecological engineering, 142 https://doi.org/10.1016/j.ecoleng.2019.105611, 2020.

Sun, W.Y., Shao, Q.Q., Liu, J.Y.: Soil erosion and its response to the changes of precipitation and vegetation cover on the Loess Plateau, JOURNAL OF GEOGRAPHICAL SCIENCES, 23(6) 1091-1106, 2013.

Syvitski, J.P.M., Alcott, J.M.: RIVER3: simulation of water and sediment river discharge from climate and drainage basin variables Comput.Geosci., 21, 89-151, 1995.

Takken, I., Beuselinck, L., Nachtergaele, J., Govers, G., Poesen, J., Degraer, G.:Spatial evaluation of a physically-based distributed erosion model (LISEM) CATENA, 37, 431-447, 1999.

Tang, C., Liu, Y., Li, Z., Guo, L., Xu, A., Zhao, J.: Effectiveness of vegetation cover pattern on regulating soil erosion and runoff generation in red soil environment, southern China, Ecological Indicators, 129, 107956 https://doi.org/10.1016/j.ecolind.2021.107956, 2021.

Thomas, R. B.: Monitoring baseline suspended sediment in forested basins: the effects of sampling on suspended sediment rating curves, Hydrological Sciences Journal, 33,5- 10, 1988.

USDA-Staff. 2019. Rainfall intensity summarisation tool (RIST) in: https://www.ars.usda.gov/southeast-area/oxford-ms/national-sedimentation-laboratory/watershed-physical-processes-research/research/rist (Accessed in January, 2020)

Van Oost, K., Govers, G., Desmet, P.: Evaluating the effects of changes in landscape structure on soil erosion by water and tillage, Landscape Ecology, 15(6), 577-589 https://doi.org/10.1023/A:1008198215674, 2000.

Vaughan, A. A., Belmont, P., Hawkins, C. P., Wilcock, P.: Near-Channel Versus Watershed Controls on Sediment Rating Curves, Journal of Geophysical Research: Earth Surface, 122(10), 1901-1923 https://doi.org/10.1002/2016JF004180, 2017.

Vanmaercke, M., Zenebe, A., Poesen, J., Nyssen, J., Verstraeten, G., and Deckers, J.:Sediment dynamics and the role of flash floods in sediment export from medium-sized catchments: a case study from the semi-arid tropical highlands in northern Ethiopia, J. Soil. Sediment., 10, 611-627, 2010.

Van Rompaey, A.J.J., Verstraeten, G., van Oost, K., Govers, G., Poesen, J.: Modelling mean annual sediment yield using a distributed approach, Earth Surface Processes and Landforms,

删除: 2020.
删除: .
删除: .
删除: .
设置格式: 字体: 五号
删除: 2013.
删除: .
删除: :
删除: Smakhtin, V.U. 2001. Low flow hydrology: a revie
删除: 1995.
删除: .
设置格式: 字体: 五号, 无下划线, 字体颜色: 自动设置
删除: 1999.
设置格式: 德语(奥地利)
删除: .
删除: atena.
删除: :
删除: 2021.
删除: .
删除: .
设置格式: 字体: 五号
删除: 1988.
删除: .
删除: .
删除: .
删除: 2000.
删除: .
删除: .
设置格式: 字体: 五号
删除: Van Rompaey, A.J.J., Verstraeten, G., van Oost, K..
删除: 2017.
删除: .
删除: .
设置格式: 字体: 五号

26,1221-1236, 2002.

Wang, J., Shi, X., Li, Z., Zhang, Y., Liu, Y., Peng, Y.:Responses of runoff and soil erosion to planting pattern, row direction, and straw mulching on sloped farmland in the corn belt of northeast China, Agricultural Water Management, 253(December 2020), 106935,https://doi.org/10.1016/j.agwat.2021.106935, 2021

Wang, L.J., Zhang, G.H., Wang, X., Li, X.Y.:Hydraulics of overland flow influenced by litter incorporation under extreme rainfall, Hydrological Processes, 33(5), 737-747, 2019.

Wang, S.P., McVicar, Tim R., Zhang, Z.Q., Brunner, T., Strauss, P.: Globally partitioning the simultaneous impacts of climate-induced and human-induced changes on catchment streamflow: A review and meta-analysis, Journal of Hydrology,https://doi.org/10.1016/j.jhydrol.2020.125387, 2020.

Warrick, J.A., Rubin, D. M.:Suspended-sediment rating curve response to surbanization and wildfire, Santa Ana River, California, Journal of Geophysical Research, 112, F02018, doi:10.1029/2006JF000662, 2007.

Wei, W., Chen, L., Fu, B., Huang, Z., Wu, D., Gui, L.:The effect of land uses and rainfall regimes on runoff and soil erosion in the semi-arid loess hilly area, China, Journal of Hydrology, 335, 247-258, 2007.

Yao, J.J., Cheng, J.H., Zhou, Z.D., Sun, L., Zhang, H.J.: Effects of herbaceous vegetation coverage and rainfall intensity on splash characteristics in northern China,CATENA, 167, 411-421, 2018.

Zhang, G.H., Liu, G.B., Wang, G.L., Wang, Y.X.:Effects of vegetation cover and rainfall intensity on sediment-associated nitrogen and phosphorus losses and particle size composition on the Loess Plateau, Journal of Soil and Water Conservation, 66(3),192-200, 2011.

Zhang, X.A., She, D., L., Hou, M., T., Wang, G.B., Liu, Y.: Understanding the influencing factors (precipitation variation, land use changes and check dams) and mechanisms controlling changes in the sediment load of a typical Loess watershed, China, Ecological Engineering, 163,https://doi.org/10.1016/j.ecoleng.2021.106198, 2021.

Zhang, X.C., Nearing, M.A.: Impact of climate change on soil erosion, runoff, and wheat productivity in central Oklahoma,CATENA, 61,185-195, 2005.

Zhang, Y., Xu, C., & Xia, M.: Can land consolidation reduce the soil erosion of agricultural land in hilly areas? Evidence from Lishui district, Nanjing city, Land, 10(5),https://doi.org/10.3390/land10050502, 2021.

删除: Wang, L.J., Zhang, G.H., Wang, X., Li, X.Y.
删除: 2021.
设置格式: 字体: 五号, 无下划线, 字体颜色: 自动设置
删除: .
删除: .
设置格式: 字体: 五号
设置格式: 字体: 五号, 无下划线, 字体颜色: 自动设置
设置格式: 字体: 五号, 无下划线, 字体颜色: 自动设置
删除: 2020.
删除: .
删除: .
设置格式: 字体: 五号
删除: , 2007.
设置格式: 字体: 五号, 无下划线, 字体颜色: 自动设置
删除: .
删除: .
删除: 2007.
设置格式: 字体: 五号, 无下划线, 字体颜色: 自动设置
删除: .
删除: .
删除: .
删除: 2018.
删除: .
删除: Catena
删除: :
删除: 2011.
设置格式: 字体: 五号, 无下划线, 字体颜色: 自动设置
删除: .
删除: :
删除: 2005.
删除: .
删除: Catena
删除: :
删除: Zhang, X.A., She, D., L., Hou, M., T., Wang, G.B.,